Electronic Transactions on Numerical Analysis.
Volume 65, pp. 441–478, 2026.

ISSN 1068–9613.
DOI: 10.1553/etna_vol65s441

ETNA
Kent State University and
Johann Radon Institute (RICAM)

CAPUTO FRACTIONAL-ORDER MODEL OF MEASLES AND REYE'S SYNDROME: INSIGHTS FROM UK SURVEILLANCE DATA ON STABILITY AND BIFURCATION*

ESEN KAYA†, FATMA ÖZKÖSE‡, AND M. TAMER ŞENEL§

Abstract. This paper proposes a fractional-order compartmental S-V-I-R-M model to investigate the transmission dynamics of measles and the potential occurrence of Reye's syndrome associated with aspirin use during infection. The model is formulated using the Caputo fractional derivative in order to incorporate memory and hereditary effects that are not captured by classical integer-order models, thereby providing a more realistic representation of epidemic dynamics. Fundamental qualitative properties of the model, including existence, uniqueness, positivity, and boundedness of solutions are rigorously established. The basic reproduction number is derived, and all equilibrium points are identified. A local stability analysis of the disease-free and endemic equilibria is performed by means of fractional-order stability theory. Furthermore, a detailed bifurcation analysis is conducted, revealing the presence of both forward and backward bifurcations. The results demonstrate that the fractional order significantly influences stability thresholds and the bifurcation behavior, thereby altering disease persistence conditions. Model parameters are estimated using measles incidence data and vaccination coverage reported by the UK Health Security Agency for the period 2019–2023 based on a 21-month observational dataset. Numerical simulations are carried out to assess the impact of public health interventions, including increased vaccination coverage and reduced aspirin use among infected individuals. The results demonstrate that the combined intervention strategy is more effective than either intervention used separately in suppressing disease transmission and reducing sustained outbreaks.

Key words. fractional differential equations, Caputo derivative, measles model, Reye's syndrome, bifurcation analysis, parameter estimation

AMS subject classifications. 34A08, 34D20, 37G10, 92D30

1. Introduction.

The measles virus, a member of the *Paramyxoviridae* family, remains a major public health concern despite the availability of an effective vaccine [37]. It continues to rank among the leading causes of morbidity and mortality in children under five, especially in regions with limited vaccination coverage. Severe complications—including pneumonia, diarrhea, laryngotracheobronchitis, otitis media, and, rarely, subacute sclerosing panencephalitis (SSPE)—remain significant contributors to disease burden [37]. Additionally, aspirin use during febrile viral infections may trigger Reye's syndrome, a rare but severe complication primarily affecting children, emphasizing the importance of behavioral factors in disease outcomes [20, 23, 34].

Measles outbreaks are largely driven by the virus's extraordinary contagiousness via direct contact, respiratory droplets, or airborne transmission [38]. Herd immunity exceeding 95% is necessary to interrupt transmission, and, given that humans are the sole natural reservoir and the virus has a single stable serotype, eradication is biologically feasible [7]. However, malnutrition, vitamin A deficiency, and inadequate vaccination coverage hinder elimination efforts [37].

Unlike classical integer-order epidemic models, fractional-order differential equations provide a natural mathematical framework for incorporating memory and hereditary effects into disease dynamics. In infectious diseases such as measles, the current number of infected

*Received January 2, 2026. Accepted May 13, 2026. Published online on August 18, 2026. Recommended by Christian Vergara.
†Corresponding author. Institute of Science, Erciyes University, 38039 Kayseri, Türkiye (es.turk.38@hotmail.com).
‡Department of Economics, Abdullah Gül University, Kayseri, Türkiye (fatma.ozkose@agu.edu.tr).
§Department of Mathematics, Faculty of Science, Erciyes University, Kayseri, Türkiye (senel@erciyes.edu.tr).

ETNA
Kent State University and
Johann Radon Institute (RICAM)

individuals may depend not only on the present state but also on the cumulative history of previous exposures, delayed immune response, vaccination history, and treatment-related complications. Therefore, the Caputo fractional derivative offers a more realistic representation of epidemic evolution than standard models by allowing the past states of the system to influence its current behavior.

Mathematical modeling has become an essential tool for understanding and predicting epidemic dynamics. Traditional integer-order models, while useful, assume a Markovian behavior, neglecting memory effects inherent in biological systems [1, 3, 24, 40]. Fractional-order differential equations, particularly those employing the Caputo derivative, overcome this limitation by incorporating history-dependent dynamics, capturing effects such as delayed immune responses, variable infectious periods, and treatment-related complications [30, 31, 39]. In this context, the physical interpretation of the fractional derivative reflects the cumulative influence of past exposures and interventions on current transmission and recovery rates.

Although several classical measles transmission models have been proposed in the literature, studies involving fractional-order formulations that simultaneously investigate stability, bifurcation behavior, and fitting to real data remain relatively limited. In particular, the role of fractional order in altering epidemic thresholds and the long-term disease persistence has not been sufficiently explored in the context of measles and Reye's syndrome.

In recent years, fractional-order epidemic models have attracted increasing attention due to their ability to incorporate memory effects that are not captured by classical integer-order formulations. In the context of measles dynamics, fractional-order modeling has been employed to better describe the persistence and temporal evolution of the disease. For example, a Caputo fractional-order compartmental model for measles infection was proposed in which the existence of solutions, equilibrium points, and stability properties were analyzed, and the impact of the fractional order on disease dynamics was demonstrated through numerical simulations. More recently, the classical SEIR measles model has been extended to a Caputo fractional-order framework, in which numerical investigations have revealed that variations in the fractional order significantly affect outbreak patterns, peak infection levels, and the long-term behavior of the system. Although these studies clearly demonstrate the relevance of fractional-order approaches in modeling measles transmission, analyses that comprehensively examine stability characteristics and Hopf bifurcation behavior within a Caputo fractional-order framework remain relatively limited. This observation provides the main motivation for the present study [5, 9].

A recent study by Naik and co-authors [5] further confirmed the effectiveness of Caputo fractional-order SEIR formulations for measles transmission, demonstrating that variations in the fractional order significantly influence numerical stability and epidemic evolution. This motivates the present investigation of stability thresholds and bifurcation behavior in the proposed S-V-I-R-M framework.

Recent studies have further strengthened the role of fractional-order epidemic modeling in capturing complex disease transmission mechanisms with memory effects. For instance, fractional-order models have been successfully applied to pneumonia transmission with vaccination and reinfection [8], COVID-19 epidemic dynamics incorporating Mittag-Leffler kernels and bifurcation analysis [22], and epidemic systems analyzed via a fixed-point theory and advanced numerical techniques [6]. These contributions provide both theoretical and computational support for the effectiveness of Caputo fractional derivatives in describing infectious disease dynamics.

Beyond infectious disease dynamics, fractional-order differential equations have also been successfully applied to other complex biomedical systems. For example, Özköse et

ETNA
Kent State University and
Johann Radon Institute (RICAM)

al. [32] developed a mathematical model of patient-derived lung cancer stem cells using fractional-order derivatives and demonstrated that memory-dependent formulations provide a more realistic representation of cellular proliferation and biological interactions. This study further supports the applicability of Caputo fractional-order models in capturing hereditary and nonlocal effects in complex health-related processes, thereby strengthening the methodological basis of the present work.

Moreover, Das et al. [11] analyzed a breast cancer model with discrete-time delay and demonstrated that time-delay effects significantly influence the stability and bifurcation structures of the system. Their results support the idea that incorporating memory-related mechanisms, either through delay terms or fractional derivatives, yields a more realistic representation of complex biological processes.

More recently, El-Mesady et al. [16] developed a fractional-order epidemiological model for tuberculosis transmission incorporating prevention and isolation control measures. Their study established the existence, positivity, boundedness, local stability, and bifurcation properties of the model, while also demonstrating the effectiveness of combined control strategies in reducing disease spread. These findings support the applicability of Caputo fractional-order formulations and optimal intervention frameworks to complex infectious disease dynamics.

Recent advances in fractional-order epidemic modeling have also addressed nonlinear phenomena such as stability changes, bifurcations, and oscillatory dynamics, with [21, 42] providing foundational results on Hopf bifurcation in fractional-order systems.

Moreover, recent studies on stability and bifurcation analysis in fractional and population dynamic systems [27, 28] further motivate the present work, particularly in exploring threshold behavior, endemic persistence, and oscillatory transitions in measles transmission dynamics.

The main objective of this study is to develop and analyze a Caputo fractional-order S-V-I-R-M model describing measles transmission together with aspirin-associated Reye's syndrome dynamics. The proposed model aims to investigate existence, uniqueness, positivity, stability properties, and bifurcation behavior while evaluating the impact of public health interventions using real surveillance data from the United Kingdom.

Furthermore, the proposed fractional-order framework provides a flexible and realistic tool for evaluating intervention strategies such as vaccination campaigns and behavioral control measures, thereby offering practical insights for public health decision-making.

The model is calibrated using real measles case data and vaccination coverage from the UK Health Security Agency (2019–2023) [14, 26, 29]. Numerical simulations are performed to evaluate the predictive behavior of the fractional-order model and to assess the impact of public health interventions, including enhanced Measles-Mumps-Rubella (MMR) vaccination coverage, reduced aspirin use among febrile children, and targeted vaccination in high-incidence regions [2, 15]. The results confirm that the fractional-order formulation provides a more realistic representation of epidemic dynamics compared to the classical integer-order model.

In summary, this work contributes a generalizable framework that bridges fractional calculus and real-world epidemiological data, offering both theoretical insights and practical guidance for evidence-based disease control. Following the formulation of the proposed model, its existence and uniqueness properties are established. Equilibrium points are subsequently identified, offering conditions for disease persistence or eradication. Section 2 provides foundational definitions in fractional calculus, while Section 3 introduces the fractional-order measles model. Existence and uniqueness results are presented in Section 4. Section 5 analyzes equilibrium points. Section 6 investigates the positivity and boundedness of solutions. Section 7 presents a sensitivity analysis of the basic reproduction number. Local and global stability analyses are discussed in Sections 8 and 9, respectively. Numerical methods are described in Section 10, simulation results in Section 11, followed by parameter estimation

ETNA
Kent State University and
Johann Radon Institute (RICAM)

in Section 12. Section 13 presents the bifurcation analysis of the proposed system. Finally, Section 14 concludes the study.

2. Preliminaries.

DEFINITION 2.1 ([36]). *The fractional integral of order $\vartheta > 0$ of a function $f(t)$ $(t > 0)$ is given by*

$$I_{\vartheta} f(t) = \frac{1}{\Gamma(\vartheta)} \int_0^x (x-t)^{\vartheta-1} f(t) dt, \qquad x > 0,$$

where $\Gamma(.)$ is the Gamma function.

DEFINITION 2.2 ([36]). *The Caputo fractional derivative of order $\vartheta > 0$ of a function $f : (0, \infty) \to \mathbb{R}$ is represented by*

$${}_0^C D_t^{\vartheta} f(t) = \begin{cases} \frac{1}{\Gamma(n-\vartheta)} \int_0^t \frac{(d/d\tau)^n f(\tau)}{(t-\tau)^{\vartheta-n+1}} d\tau, & 0 \le n-1 < \vartheta < n, n = [\vartheta], n \in \mathbb{N}, \\ \left(\frac{d}{dt}\right)^n f(t), & \vartheta = n, n \in \mathbb{N}. \end{cases}$$

LEMMA 2.3 ([36]). *The Laplace transform (LT) of a function $f(t)$ of order $\vartheta > 0$ is given by*

$$L[{}_0^C D_t^{\vartheta} f(t)] = s^{\vartheta} F(s) - \sum_{v=0}^{n-1} f^{(v)}(0) s^{\vartheta-v-1}.$$

LEMMA 2.4 ([36]). *The Laplace transform (LT) of $f(t) = t^{\vartheta_1-1} E_{\vartheta,\vartheta_1}(\pm\omega t^{\vartheta})$, with the Mittag-Leffler function $E_{\vartheta,\vartheta_1}$, is given by*

$$L[t^{\vartheta_1-1} E_{\vartheta,\vartheta_1}(\pm\omega t^{\vartheta})] = \frac{s^{\vartheta-\vartheta_1}}{s^{\vartheta} \pm \omega}.$$

THEOREM 2.5 ([4, 35, 36]). *Consider the fractional-order system*

$$\frac{d^{\vartheta} X}{dt^{\vartheta}} = f(X), \qquad X(0) = X_0,$$

with $\alpha \in (0, 1]$ and $X \in \mathbb{R}^n$. The zeros of the function $f(X^*) = 0$ are the equilibrium points of the system (3.1), and these equilibrium points are

(1) asymptotically stable $\iff$ the eigenvalues λ_i of the Jacobian matrix $J(X^*)$ satisfy $|\arg(\lambda_i)| > \frac{\vartheta\pi}{2}, \forall i, i = 1, 2, \ldots, n$;

(2) unstable $\iff$ $\exists i$ such that the corresponding eigenvalue λ_i of $J(X^*)$ satisfies $|\arg(\lambda_i)| < \frac{\vartheta\pi}{2}, i = 1, 2, \ldots, n$.

THEOREM 2.6 ([36]). *Consider the polynomial equation*

$$P(\lambda) = \lambda^n + a_1\lambda^{n-1} + ... + a_{n-1}\lambda + a_n = 0,$$

and let λ_i denote the zeros.

(1) For $n = 1$, the condition for $|\arg(\lambda_i)| > \frac{\vartheta\pi}{2}$ is

$$a_1 > 0.$$

ETNA
Kent State University and
Johann Radon Institute (RICAM)

(2) For $n = 2$, the conditions for $|\arg(\lambda_i)| > \frac{\vartheta\pi}{2}$ are either

$$a_1 > 0, \qquad a_2 > 0$$

or

$$a_1 < 0, \quad 4a_2 > a_1^2, \quad \left|\tan^{-1}(4a_2 > a_1^2)\right| > \frac{\vartheta\pi}{2}.$$

(3) For $n = 3$, the conditions for $|\arg(\lambda_i)| > \frac{\vartheta\pi}{2}$ are

$$a_1 > 0, \qquad a_3 > 0, \quad \textit{and} \quad a_1 a_2 > a_3,$$

(4) For $n = 4$, the conditions for $|\arg(\lambda_i)| > \frac{\vartheta\pi}{2}$ are

$$a_1 > 0, \qquad a_3 > 0, \qquad a_4 > 0, \quad \textit{and} \quad a_1 a_2 a_3 > a_3^2 + a_1^2 a_4,$$

(5) For $n = 5$, the conditions for $|\arg(\lambda_i)| > \frac{\vartheta\pi}{2}$ are the Routh-Hurwitz conditions [19]

$$\begin{aligned} a_i &> 0, \qquad i = 1, 2, 3, 4, 5, \\ a_1 a_2 a_3 &> a_3^2 + a_1^2 a_4, \qquad \textit{and} \\ (a_1 a_4 - a_5)\left(a_1 a_2 a_3 - a_3^2 - a_1^2 a_4\right) &> a_5 \left(a_1 a_2 - a_3\right)^2 + a_1 a_5^2. \end{aligned}$$

3. Mathematical model. Mathematical models can be used to predict the spread of infectious diseases and the effects of aspirin use on this disease. Many diseases can be treated and their spread halted using mathematical models. Our aim is to monitor the spread of the disease with the help of these mathematical models and to assist science by observing the impact of this disease on people. Measles, whose prevalence has increased with external migration to our country in recent years, causes the death of many people. To examine the spread of measles and the effects of aspirin on this disease, we consider five subclasses: susceptible individuals, vaccinated individuals, infected individuals, recovered individuals, and individuals who developed Reye's syndrome as a result of aspirin use while ill. We denote susceptible individuals by S, vaccinated individuals by V, infected individuals by I, recovered individuals by R, individuals who developed Reye's syndrome as a result of aspirin use while infected by M, and the total population by N. The proposed fractional-order model is as follows:

$$\begin{aligned} {}_0^C D_t^\vartheta S(t) &= b^\vartheta S\left(1 - \frac{S}{K}\right) - S\left(\mu_1^\vartheta + \omega^\vartheta\right) - \frac{I\beta^\vartheta S}{N} - S(\psi_1^\vartheta + \psi_2^\vartheta), \\ {}_0^C D_t^\vartheta V(t) &= S(\psi_1^\vartheta + \psi_2^\vartheta) - \left(\mu_1^\vartheta + \tau_1^\vartheta + \tau_2^\vartheta\right) V, \\ {}_0^C D_t^\vartheta I(t) &= -I\left(\gamma^\vartheta + \delta^\vartheta + \zeta^\vartheta + \theta^\vartheta + \mu_1^\vartheta\right) + \frac{I\beta^\vartheta S}{N} + S\omega^\vartheta + \tau_1^\vartheta V, \\ {}_0^C D_t^\vartheta R(t) &= I(\gamma^\vartheta + \theta^\vartheta) + I\zeta^\vartheta\xi - \mu_1^\vartheta R + \tau_2^\vartheta V, \\ {}_0^C D_t^\vartheta M(t) &= I\zeta^\vartheta(1 - \xi) - \mu_2^\vartheta M, \end{aligned} \tag{3.1}$$

with the initial conditions

$$\begin{aligned} S(0) &= S_0 \geq 0, \qquad V(0) = V_0 \geq 0, \qquad I(0) = I_0 \geq 0, \\ R(0) &= R_0 \geq 0 \qquad M(0) = M_0 \geq 0, \end{aligned}$$

where $t \geq 0$ and ϑ $(0 < \vartheta \leq 1)$ is the order of the model.

ETNA
Kent State University and
Johann Radon Institute (RICAM)

Equation (3.1) represents a Caputo fractional-order compartmental model that describes the transmission dynamics of measles with vaccination and disease-related complications. The state variables $S(t)$, $V(t)$, $I(t)$, $R(t)$, and $M(t)$ denote the populations of susceptible, vaccinated, infected, recovered individuals, and individuals experiencing severe complications, respectively.

The first equation describes the dynamics of the susceptible population. The term $b^{\vartheta} S\left(1-\frac{S}{K}\right)$ represents the intrinsic growth of susceptible individuals under limited resources, where K is the carrying capacity. The term $S(\mu_1^{\vartheta}+\omega^{\vartheta})$ accounts for natural mortality and the transition of susceptible individuals due to exposure-related processes, while the bilinear incidence term $\frac{\beta^{\vartheta} IS}{N}$ models disease transmission through effective contact between susceptible and infected individuals. The vaccination-related terms $S(\psi_1^{\vartheta}+\psi_2^{\vartheta})$ describe the transfer of susceptible individuals to the vaccinated class.

The second equation governs the vaccinated population. The class $V(t)$ increases due to vaccination of susceptible individuals and decreases because of natural mortality and vaccine waning or loss of immunity, represented by the rates τ_1^{ϑ} and τ_2^{ϑ}.

The third equation characterizes the infected population. New infections arise from effective contact between susceptible and infected individuals as well as through transitions from the vaccinated class. The removal terms correspond to recovery, disease-induced mortality, natural death, and progression to severe complications.

The fourth equation describes the recovered population, which increases through the recovery of infected individuals and immunity acquisition from the vaccinated class. The parameter ξ represents the proportion of infected individuals who recover without developing severe complications, while the class decreases due to natural mortality.

The final equation models the dynamics of individuals experiencing severe complications. This population increases from a fraction $(1-\xi)$ of infected individuals and decreases due to complication-related mortality at the rate μ_2^{ϑ}.

From a biological point of view, the proposed fractional-order S-V-I-R-M model provides a more realistic framework then standard models for describing disease transmission dynamics by incorporating memory and hereditary effects through the Caputo fractional derivative. Unlike classical integer-order models, where the evolution of each compartment depends only on its current state, the fractional-order formulation accounts for the entire history of the system. This is particularly relevant in infectious disease dynamics, where past exposures, immune responses, and delayed effects of vaccination influence the current progression of the disease.

Within this framework, the susceptible population is influenced not only by current interactions but also by past epidemic conditions. The vaccinated class reflects both immediate protection and time-dependent waning immunity. The infected class captures memory-dependent effects related to incubation periods and disease progression, while the recovered class incorporates delayed recovery and long-term immune response. The compartment representing individuals with severe complications accounts for delayed adverse outcomes associated with aspirin use during infection.

The fractional-order parameter ϑ acts as a memory index governing the influence of past states on the current dynamics. Smaller values of ϑ correspond to stronger memory effects, leading to slower disease evolution and prolonged persistence, whereas values approaching one recover the classical memoryless integer-order model. This provides a clear biological justification for using fractional calculus in modeling measles transmission and related complications.

The Caputo fractional derivative of order ϑ $(0<\vartheta\leq 1)$ introduces a nonlocal temporal dependence, allowing the present rate of change of each compartment to depend on its entire

ETNA
Kent State University and
Johann Radon Institute (RICAM)

history. This yields a more realistic description of epidemic evolution than classical ODE models, particularly in capturing delayed responses and long-term persistence. All model parameters are assumed to be nonnegative to ensure biological feasibility.

From a modeling perspective, dimensional consistency is essential to preserve the physical and biological interpretability of the system. Özköse et al. [33] emphasized that fractional-order models require careful parameter rescaling since the nonlocal character of fractional derivatives alters the classical temporal dimension. In the case of Caputo derivatives of order ϑ, the time dimension is effectively generalized, and parameters must be defined in fractional-order units (e.g., time$^{-\vartheta}$) to maintain dimensional homogeneity. This ensures that each term in the system remains consistently balanced and prevents biologically unrealistic interpretations. Following established approaches in fractional epidemic modeling, the present formulation guarantees dimensional consistency across all state variables and parameters. This not only supports the physical validity of the model but also enables meaningful comparison with classical integer-order systems, particularly in the analysis of stability and the long-term dynamical behavior. The definitions and biological meanings of all model parameters used in the system (3.1) are presented in Table 3.1.

TABLE 3.1
The biological meanings of the parameters.

Par.	Description
S_0	initial population of susceptible individuals
V_0	initial population of vaccinated individuals
I_0	initial population of infected individuals
R_0	initial population of recovered individuals
M_0	initial population of individuals who developed Reye's syndrome as a result of aspirin use while infected
N	total population
β	transmission rate
ω	the rate of individuals with prejudice against vaccination
τ_1	the rate of people vaccinated against measles
τ_2	the rate of people vaccinated and cured of measles
ψ_1	the rate of people who received the first dose of the measles vaccine
ψ_2	the rate of people who received the second dose of the measles vaccine
μ_1	the natural death rate of humans in the district
μ_2	death rate from Reye's syndrome
θ	the rate of those taking vitamin A supplements
b	logistic growth rate of susceptible individuals
ζ	the rate of people using aspirin during measles treatment
ξ	the rate of those who were infected, recovered, and became immune by using aspirin
γ	the recovery rate of infected individuals
δ	the death rate due to measles infection
K	carrying capacity of the population

4. Existence and uniqueness. Let us take into account the system with the initial conditions

$$S(0) = S_0, \quad V(0) = V_0, \quad I(0) = I_0, \quad R(0) = R_0, \quad M(0) = M_0.$$

ETNA
Kent State University and
Johann Radon Institute (RICAM)

It is possible to express the system as

$$\begin{cases} {}_0^C D_t^{\vartheta} X(t) = A_1 X(t) + S(t) A_2 X(t) + V(t) A_3 X(t), & t > 0, \\ X(0) = X_0, \end{cases} \tag{4.1}$$

where

$$X(t) = \begin{bmatrix} S(t) \\ V(t) \\ I(t) \\ R(t) \\ M(t) \end{bmatrix}, \qquad X(0) = \begin{bmatrix} S(0) \\ V(0) \\ I(0) \\ R(0) \\ M(0) \end{bmatrix},$$

$$A_1 = \begin{bmatrix} -(\mu_1^{\vartheta} + \omega^{\vartheta} + \psi_1^{\vartheta} + \psi_2^{\vartheta} - b^{\vartheta}) & 0 & 0 & 0 & 0 \\ \psi_1^{\vartheta} + \psi_2^{\vartheta} & -(\tau_1^{\vartheta} + \tau_2 + \mu_1^{\vartheta}) & 0 & 0 & 0 \\ \omega^{\vartheta} & \tau_1^{\vartheta} & -(\gamma^{\vartheta} + \delta^{\vartheta} + \mu_1^{\vartheta} + \theta^{\vartheta} + \zeta) & 0 & 0 \\ 0 & \tau_2^{\vartheta} & \gamma^{\vartheta} + \theta^{\vartheta} & -\mu_1^{\vartheta} & 0 \\ 0 & 0 & \zeta^{\vartheta} & 0 & -\mu_2^{\vartheta} \end{bmatrix},$$

$$A_2 = \begin{bmatrix} 0 & 0 & 0 & 0 & 0 \\ 0 & 0 & 0 & 0 & 0 \\ 0 & 0 & 0 & 0 & 0 \\ 0 & 0 & \zeta^{\vartheta}\xi I & 0 & 0 \\ 0 & 0 & -\zeta^{\vartheta}\xi I & 0 & 0 \end{bmatrix}, \qquad A_3 = \begin{bmatrix} -\frac{b^{\vartheta}}{K} & 0 & -\frac{\beta^{\vartheta}}{N} & 0 & 0 \\ 0 & 0 & 0 & 0 & 0 \\ 0 & 0 & \frac{\beta^{\vartheta}}{N} & 0 & 0 \\ 0 & 0 & 0 & 0 & 0 \\ 0 & 0 & 0 & 0 & 0 \end{bmatrix}.$$

In view of verifying existence and uniqueness of solutions, we give the following definitions:

DEFINITION 4.1 ([30]). *Let $C^*[0,\tau]$ be the class of continuous column vectors $X(t)$ whose components $S, V, I, R, M \in C^*[0,\tau]$ are in the class of continuous functions on the interval $[0,\tau]$. The norm of $X \in C^*[0,\tau]$ is*

$$\begin{aligned} \|X\| = \sup_t \left|e^{-Nt} S(t)\right| + \sup_t \left|e^{-Nt} V(t)\right| + \sup_t \left|e^{-Nt} I(t)\right| \\ + \sup_t \left|e^{-Nt} R(t)\right| + \sup_t \left|e^{-Nt} M(t)\right|; \end{aligned}$$

when $t > \psi \geq m$, we write $C_{\psi}^*[0,\tau]$ and $C_{\psi}[0,\tau]$.

DEFINITION 4.2 ([30]). *Let*

$$\mathbb{R}_+^5 = \left\{\zeta(t) \in \mathbb{R}^5 : \zeta(t) \geq 0\right\}.$$

Then $X \in C^*[0,\tau]$ is a solution of the initial value problem (IVP)(4.1) if

(1) $(t, X(t)) \in D, t \in [0,\tau]$, where $D = [0,\tau] \times K$,

$$K = \left\{(S,V,I,R,M) \in \mathbb{R}_+^5 : |S| \leq p, |V| \leq r, |I| \leq w, |R| \leq q, |M| \leq s\right\},$$

and p, r, w, q, s are positive constants, and

(2) $X(t)$ satisfies (4.1).

ETNA
Kent State University and
Johann Radon Institute (RICAM)

We can now prove existence and uniqueness:

THEOREM 4.3. *The IVP* (4.1) *has a unique solution* $X \in C^*[0,\tau]$.

Proof. For $0 < \vartheta \leq 1$, the fractional-order system (4.1) can be written in the equivalent integral form

$$X(t) = X(0) + I^{\vartheta}\left(A_1X(t) + S(t)A_2X(t) + V(t)A_3X(t)\right). \tag{4.2}$$

Here, A_1, A_2, and A_3 are constant matrices, and $|\cdot|$ denotes the induced matrix norm. Define the operator $F : C^*[0,\tau] \to C^*[0,\tau]$ by

$$FX(t) = X(0) + I^{\vartheta}\left(A_1X(t) + S(t)A_2X(t) + V(t)A_3X(t)\right). \tag{4.3}$$

Let $X, Y \in C^*[0,\tau]$. Let $X, Y \in C^*[0,\tau]$. Using the weighted norm

$$|X| = \sup_{0\leq t\leq\tau} e^{-Gt}|X(t)|,$$

where $G > 0$ is a positive constant, we obtain

$$|FX - FY| \leq \frac{1}{\Gamma(\vartheta)} \sup_{0\leq t\leq\tau} \int_0^t \Big[(t-s)^{\vartheta-1}e^{-G(t-s)}\left(|A_1| + |S(s)|\,|A_2| + |V(s)|\,|A_3|\right) \times e^{-Gs}|X(s) - Y(s)|\Big]\, ds.$$

Since $|S(t)| \leq p$ and $|V(t)| \leq r$ on $[0,\tau]$, it follows that

$$|FX - FY| \leq \left(|A_1| + p|A_2| + r|A_3|\right)|X - Y| \sup_{0\leq t\leq\tau} \frac{1}{\Gamma(\vartheta)} \int_0^t (t-s)^{\vartheta-1}e^{-G(t-s)}\, ds.$$

By the change of variable $u = t - s$, we have

$$\frac{1}{\Gamma(\vartheta)} \int_0^t (t-s)^{\vartheta-1}e^{-G(t-s)}\, ds = \frac{1}{\Gamma(\vartheta)} \int_0^t u^{\vartheta-1}e^{-Gu}, du \leq \frac{1}{G^{\vartheta}}.$$

Here, G^{ϑ} denotes the ϑ-th power of the positive constant G. Consequently,

$$|FX - FY| \leq \frac{|A_1| + p|A_2| + r|A_3|}{G^{\vartheta}}|X - Y|.$$

Choose $G > 0$ sufficiently large such that

$$\frac{|A_1| + p|A_2| + r|A_3|}{G^{\vartheta}} < 1.$$

Then there exists a constant $0 < q < 1$ such that

$$|FX - FY| \leq q|X - Y|.$$

Hence, F is a contraction on $C^*[0,\tau]$. By the Banach fixed-point theorem, F has a unique fixed point in $C^*[0,\tau]$. Therefore, the integral equation (4.2) has a unique solution $X \in C^*[0,\tau]$. It remains to show that the integral equation (4.2) is equivalent to the original fractional initial value problem (4.1). From (4.2),

$$X(t) - X(0) = I^{\vartheta}\left(A_1X(t) + S(t)A_2X(t) + V(t)A_3X(t)\right).$$

ETNA
Kent State University and
Johann Radon Institute (RICAM)

Applying the Caputo fractional derivative ${}^{C}D_t^{\vartheta}$ to both sides and using the identity

$$ {}^{C}D_t^{\vartheta} I^{\vartheta} f(t) = f(t), $$

we obtain

$$ {}^{C}D_t^{\vartheta} X(t) = A_1 X(t) + S(t) A_2 X(t) + V(t) A_3 X(t). $$

Moreover, setting $t = 0$ in (4.2) gives

$$ X(0) = X_0. $$

Thus, the integral equation (4.2) is equivalent to the IVP (4.1). Therefore, the IVP (4.1) admits a unique solution $X \in C^*[0, \tau]$. □

5. Equilibrium points and their stability. To calculate the equilibria of the system (3.1), let

$$ {}_0^C D_t^{\vartheta} S(t) = 0, \qquad {}_0^C D_t^{\vartheta} V(t) = 0, \qquad {}_0^C D_t^{\vartheta} I(t) = 0, $$
$$ {}_0^C D_t^{\vartheta} R(t) = 0, \qquad {}_0^C D_t^{\vartheta} M(t) = 0. $$

Thus,

$$ \begin{aligned}
&{}_0^C D_t^{\vartheta} S(t) = b^{\vartheta} S \left(1 - \frac{S}{K}\right) - S\left(\mu_1^{\vartheta} + \omega^{\vartheta}\right) - \frac{I \beta^{\vartheta} S}{N} - S(\psi_1^{\vartheta} + \psi_2^{\vartheta}) = 0, \\
&{}_0^C D_t^{\vartheta} V(t) = S(\psi_1^{\vartheta} + \psi_2^{\vartheta}) - \left(\mu_1^{\vartheta} + \tau_1^{\vartheta} + \tau_2^{\vartheta}\right) V = 0, \\
&{}_0^C D_t^{\vartheta} I(t) = -I\left(\gamma^{\vartheta} + \delta^{\vartheta} + \zeta^{\vartheta} + \theta^{\vartheta} + \mu_1^{\vartheta}\right) + \frac{I \beta^{\vartheta} S}{N} + S\omega^{\vartheta} + \tau_1^{\vartheta} V = 0, \\
&{}_0^C D_t^{\vartheta} R(t) = I(\gamma^{\vartheta} + \theta^{\vartheta}) + I\zeta^{\vartheta}\xi - \mu_1^{\vartheta} R + \tau_2^{\vartheta} V = 0, \\
&{}_0^C D_t^{\vartheta} M(t) = I\zeta^{\vartheta}(1 - \xi) - \mu_2^{\vartheta} M = 0.
\end{aligned} $$

Then there are three equilibrium points:

$$ E_1 = (0, 0, 0, 0, 0), \qquad E_2 = (a^*, b^*, c^*, d^*, e^*), \qquad E_3 = (k^*, l^*, m^*, n^*, o^*). \tag{5.1} $$

The formulas for E_2, E_3 can be computed, e.g., by symbolic computations; however, since the expressions are rather long (over multiple pages), we do not state them explicitly.

6. Positivity and boundedness. In this section, the positivity and boundedness of the solution of the model (3.1) are examined. Let

$$ \zeta(t) = [S(t), V(t), I(t), R(t), M(t)]^T. $$

Let us recall a lemma that will be used to verify the nonnegativity of the solution of the model (3.1).

ETNA
Kent State University and
Johann Radon Institute (RICAM)

LEMMA 6.1 (Generalized Mean Value Theorem [36]). *Assume that*

$$w(t) \in C[a,b] \quad \textit{and} \quad {}_0^C D_t^{\vartheta} w(t) \in C[a,b], \quad \textit{for } 0 < \vartheta \leq 1.$$

Then

$$w(t) = w(a) + \frac{1}{\Gamma(\vartheta)} {}_0^C D_t^{\vartheta} w(\tau)(t-a)^{\vartheta},$$

where $0 \leq \tau \leq t, \forall t \in (a,b]$.

REMARK 6.2. If $w \in C[a,b]$ and ${}_0^C D_t^a w(t) \geq 0$, for all $t \in (a,b]$, then the function $w(t)$ is non-increasing for all $t \in (a,b]$.

THEOREM 6.3. *The model* (3.1) *with the initial conditions has a bounded solution in* $\mathbb{R}_+^5$.

Proof.

$$\begin{aligned}
{}_0^C D_t^{\vartheta} S\big|_{S=0} &= 0 \geq 0,\\
{}_0^C D_t^{\vartheta} V\big|_{V=0} &= S(\psi_1^{\vartheta} + \psi_2^{\vartheta}) \geq 0,\\
{}_0^C D_t^{\vartheta} I\big|_{I=0} &= S\omega^{\vartheta} + \tau_1^{\vartheta} V \geq 0,\\
{}_0^C D_t^{\vartheta} R\big|_{R=0} &= I(\gamma^{\vartheta} + \theta^{\vartheta}) + I\zeta^{\vartheta}\xi + \tau_2^{\vartheta} V \geq 0,\\
{}_0^C D_t^{\vartheta} M\big|_{M=0} &= I\zeta^{\vartheta}(1-\xi) \geq 0.
\end{aligned} \tag{6.1}$$

If $(S(0), V(0), I(0), R(0), M(0)) \in \mathbb{R}_+^5$, then from (6.1) and Remark 6.2, the solution of the model (3.1) can only lie above the hyperplanes $S(t) = 0, V(t) = 0, I(t) = 0, R(t) = 0$, and $M(t) = 0$. This result demonstrates that the region $\mathbb{R}_+^5$ constitutes a positively invariant set. □

THEOREM 6.4. *The region*

$$Q = \left\{ S(t), V(t), I(t), R(t), M(t) \in \mathbb{R}_+^5, \quad 0 < S(t), V(t), I(t), R(t), M(t) \leq C \right\}$$

is a positive invariant set for the system (3.1).

Proof. Equations (3.1) yield the following:

$${}_0^C D_t^{\vartheta} N(t) = b^{\vartheta} S \left(1 - \frac{S}{K}\right) - \mu_1^{\vartheta}(S + V + I + R) - \mu_2^{\vartheta} M.$$

This gives

$${}_0^C D_t^{\vartheta} N(t) \leq b^{\vartheta} S + \mu_1^{\vartheta} N.$$

Consequently, summing all equations of the system (3.1) yields an upper bound for the total population $N(t)$ in the form of the following fractional differential inequality:

$${}_0^C D_t^{\vartheta} N(t) \leq \left(\mu_1^{\vartheta} + b^{\vartheta}\right) N(t),$$

which ensures that the total population remains bounded for all $t \geq 0$.

If we apply the Laplace transform, then we have

$$s^{\vartheta}\, w(s) - s^{\vartheta-1} N(0) \leq \left(\mu_1^{\vartheta} + b^{\vartheta}\right) w(s),$$

which further gives $w(N) \leq \frac{s^{\vartheta-1}}{s^{\vartheta} - b - \mu_1} N(0)$. By taking the inverse Laplace transform, we get that if $(S(t), V(t), I(t), R(t), M(t)) \in \mathbb{R}_+^5$, then

$$N(t) \leq E_{\vartheta,1}\left(-(\mu_1^{\vartheta} + b^{\vartheta}) t^{\vartheta}\right),$$

ETNA
Kent State University and
Johann Radon Institute (RICAM)

with the Mittag-Leffler function $E_{\vartheta,1}$. From its definition we obtain

$$N(t) \leq \sum_{k=0}^{\infty} \frac{\left[-(\mu_1^{\vartheta} + b^{\vartheta})t^{\vartheta}\right]^k}{\Gamma(\vartheta k + 1)}.$$

By applying the ratio test for convergence, it follows that the above series is convergent. Hence, its sum is bounded by a positive constant $C > 0$, that is,

$$N(t) \leq C.$$

Therefore, the state variables $S(t), V(t), I(t), R(t), M(t)$ are bounded. □

From an epidemiological perspective, the positivity of the solutions guarantees that all population compartments remain biologically meaningful throughout the evolution of the system since negative values for susceptible, vaccinated, infected, recovered, or complication-related classes are not physically interpretable. Similarly, boundedness ensures that the total population remains within realistic limits over time, thereby confirming the reliability and practical applicability of the proposed model in real epidemic scenarios.

7. Basic reproduction number. The basic reproduction number R_0 for a single infected person is a threshold that indicates the total number of potential cases generated in a completely susceptible population during its transmission period. F and V are the matrices created for the new infection and the transition terms, respectively. Following the same method as in [41], the basic reproduction number is calculated as follows:

$$f = \begin{bmatrix} 0 \\ 0 \\ \frac{\beta^{\vartheta} SI}{N} \\ 0 \\ 0 \end{bmatrix}, \qquad v = \begin{bmatrix} -b^{\vartheta} S\left(1 - \frac{S}{K}\right) + S\left(\mu_1^{\vartheta} + \omega^{\vartheta}\right) + \frac{I\beta^{\vartheta} S}{N} + S(\psi_1^{\vartheta} + \psi_2^{\vartheta}) \\ -S(\psi_1^{\vartheta} + \psi_2^{\vartheta}) + \left(\mu_1^{\vartheta} + \tau_1^{\vartheta} + \tau_2^{\vartheta}\right) V \\ I\left(\gamma^{\vartheta} + \delta^{\vartheta} + \zeta^{\vartheta} + \theta^{\vartheta} + \mu_1^{\vartheta}\right) - S\omega^{\vartheta} + \tau_1^{\vartheta} V \\ -I(\gamma^{\vartheta} + \theta^{\vartheta}) - I\zeta^{\vartheta}\xi - \mu_1^{\vartheta} R + \tau_2^{\vartheta} V \\ -I\zeta^{\vartheta}(1 - \xi) + \mu_2^{\vartheta} M \end{bmatrix},$$

$$F = \begin{bmatrix} \frac{\beta^{\vartheta} S_0}{N} & 0 \\ 0 & 0 \end{bmatrix}, \qquad V = \begin{bmatrix} \gamma^{\vartheta} + \delta^{\vartheta} + \zeta^{\vartheta} + \theta^{\vartheta} + \mu_1^{\vartheta} & 0 \\ -\zeta^{\vartheta}(1 - \xi) & \mu_2^{\vartheta} \end{bmatrix}.$$

The expression for R_0 is the spectral radius of the matrix FV^{-1} and is given by

$$R_0 = \frac{\beta S_0}{N(\gamma + \delta + \zeta + \theta + \mu_1)}, \qquad S_0 = \frac{K(b - \mu_1 - \omega - \psi_1 - \psi_2)}{b},$$

thus,

$$R_0 = \frac{\beta K(b - \mu_1 - \omega - \psi_1 - \psi_2)}{bN(\gamma + \delta + \zeta + \theta + \mu_1)}.$$

7.1. Sensitivity analysis. In this section, we analyze the sensitivity of R_0 with respect to parameters that affect the reproduction number. A sensitivity measure shows the relative changes that may occur in variables due to a change in a given parameter. We have applied the same method as in [10]. Given the importance of the reproduction number in calculating disease prevalence, it is necessary to assess the sensitivities of the parameters with respect to

ETNA
Kent State University and
Johann Radon Institute (RICAM)

R_0.

$$\begin{aligned}
\frac{\partial R_0}{\partial \gamma} &= \frac{\partial R_0}{\partial \delta} = \frac{\partial R_0}{\partial \zeta} = \frac{\partial R_0}{\partial \theta} = \frac{-bN(\beta K(b-\mu_1-\omega-\psi_1-\psi_2)}{(bN(\gamma+\delta+\zeta+\theta+\mu_1))^2} < 0,\\
\frac{\partial R_0}{\partial \mu_1} &= \frac{-\beta K(bN(\gamma+\delta+\zeta+\theta+\mu_1) - bN(\beta K(b-\mu_1-\omega-\psi_1-\psi_2)}{(bN(\gamma+\delta+\zeta+\theta+\mu_1))^2} < 0,\\
\frac{\partial R_0}{\partial \omega} &= \frac{\partial R_0}{\partial \psi_1} = \frac{\partial R_0}{\partial \psi_2} = \frac{-\beta K(bN(\gamma+\delta+\zeta+\theta+\mu_1)}{(bN(\gamma+\delta+\zeta+\theta+\mu_1))^2} < 0,\\
\frac{\partial R_0}{\partial b} &= \frac{\beta K(bN(\gamma+\delta+\zeta+\theta+\mu_1) - N(\gamma+\delta+\zeta+\theta+\mu_1)\beta K(b-\mu_1-\omega-\psi_1-\psi_2)}{(bN(\gamma+\delta+\zeta+\theta+\mu_1))^2} > 0,\\
\frac{\partial R_0}{\partial K} &= \frac{\beta(b-\mu_1-\omega-\psi_1-\psi_2)bN(\gamma+\delta+\zeta+\xi+\mu_1)}{(bN(\gamma+\delta+\zeta+\theta+\mu_1))^2} > 0,\\
\frac{\partial R_0}{\partial \beta} &= \frac{K(b-\mu_1-\omega-\psi_1-\psi_2)bN(\gamma+\delta+\zeta+\theta+\mu_1)}{(bN(\gamma+\delta+\zeta+\theta+\mu_1))^2} > 0.
\end{aligned}$$

From the sensitivity analysis, it can be seen that R_0 increases with the parameters b, K, β and decreases with $\gamma, \delta, \zeta, \theta, \mu_1, \omega, \psi_1, \psi_2$. This indicates that in order to reduce disease outbreaks, parameters with negative negative sensitivity indices should be maximized.

8. Local stability of the equilibria. The necessary conditions for the stability of the equilibrium points are summarized below.

THEOREM 8.1. *Let E_1 denote the disease-free equilibrium (DFE) of the system (3.1). Then, the equilibrium point E_1 is unstable.*

Proof. The Jacobian matrix of system (3.1) evaluated at the disease-free equilibrium E_1 is given by

$$J(E_1) = \begin{bmatrix}
b^\vartheta - \mu_1^\vartheta - \omega^\vartheta & 0 & 0 & 0 & 0\\
\psi_1^\vartheta + \psi_2^\vartheta & -(\mu_1^\vartheta + \tau_1^\vartheta + \tau_2^\vartheta) & 0 & 0 & 0\\
\omega^\vartheta & \tau_1^\vartheta & -(\zeta^\vartheta + \delta^\vartheta + \mu_1^\vartheta + \gamma^\vartheta + \theta^\vartheta) & 0 & 0\\
0 & \tau_2^\vartheta & \zeta^\vartheta\xi + \gamma^\vartheta + \theta^\vartheta & -\mu_1^\vartheta & 0\\
0 & 0 & \zeta^\vartheta(1-\xi) & 0 & -\mu_2^\vartheta
\end{bmatrix}.$$

Since the Jacobian matrix is triangular, the characteristic equation is obtained directly from its diagonal entries as

$$\begin{aligned}
P(\lambda) = {} & (-\lambda-\mu_1)(-\lambda-\mu_2)(-\lambda-\mu_1-\tau_1-\tau_2)\\
& \times (b-\mu_1-\omega-\lambda)(-\gamma-\delta-\zeta-\theta-\mu_1-\lambda) = 0.
\end{aligned}$$

Hence, the eigenvalues are

$$\begin{aligned}
&\lambda_1 = -\mu_1, && \lambda_2 = -\mu_2, && \lambda_3 = -(\mu_1+\tau_1+\tau_2),\\
&\lambda_4 = b-\mu_1-\omega, && \lambda_5 = -(\gamma+\delta+\zeta+\theta+\mu_1).
\end{aligned}$$

Under biologically meaningful assumptions, all parameters are positive. Consequently, λ_1, λ_2, λ_3, and λ_5 have negative real parts, whereas λ_4 can be positive. Therefore, the disease-free equilibrium E_1 is unstable. □

THEOREM 8.2. *Let E_2 and E_3 (cf. (5.1)) be the equilibrium points of the system (3.1). If $R_0 < 1$, then E_2 and E_3 are locally asymptotically stable.*

ETNA
Kent State University and
Johann Radon Institute (RICAM)

Proof. The Jacobian matrix evaluated at E_2 is given by

$$J(E_2) = \begin{bmatrix} j_{11} & 0 & j_{13} & 0 & 0 \\ \psi_1^\vartheta + \psi_2^\vartheta & -(\mu_1^\vartheta + \tau_1^\vartheta + \tau_2^\vartheta) & 0 & 0 & 0 \\ j_{31} & \tau_1^\vartheta & j_{33} & 0 & 0 \\ 0 & \tau_2^\vartheta & \gamma^\vartheta + \theta^\vartheta + \zeta^\vartheta \xi & -\mu_1^\vartheta & 0 \\ 0 & 0 & \zeta^\vartheta(1-\xi) & 0 & -\mu_2^\vartheta \end{bmatrix},$$

where

$$\begin{aligned} j_{11} &= b^\vartheta \left(1 - \frac{2S^*}{K}\right) - (\mu_1^\vartheta + \omega^\vartheta) - \frac{I^*\beta^\vartheta}{N}, \\ j_{13} &= -\frac{S^*\beta^\vartheta}{N}, \\ j_{31} &= \omega^\vartheta + \frac{I^*\beta^\vartheta}{N}, \\ j_{33} &= -(\gamma^\vartheta + \delta^\vartheta + \zeta^\vartheta + \theta^\vartheta + \mu_1^\vartheta) + \frac{S^*\beta^\vartheta}{N}. \end{aligned}$$

Here S^*, I^*, V^* involve long formulas that are computed without much effort but which are too long to be stated here.

The characteristic polynomial can be expressed as

$$P(\lambda) = (-\lambda - \mu_1)(-\lambda - \mu_2)\left(\lambda^3 + a_1\lambda^2 + a_2\lambda + a_3\right),$$

where the coefficients a_1, a_2, and a_3 (which can be calculated straightforwardly but are omitted for brevity) are positive for $R_0 < 1$. According to the Routh–Hurwitz criteria, if

$$a_1 > 0, \quad a_3 > 0, \quad a_1 a_2 > a_3,$$

then all roots of the cubic polynomial have negative real parts. Furthermore, for a fractional-order system of order $0 < \vartheta \le 1$, Matignon's stability criterion ensures stability provided

$$|\arg(\lambda_i)| > \frac{\vartheta\pi}{2}, \qquad i = 1, \ldots, 5.$$

Hence, when $R_0 < 1$, all eigenvalues satisfy the fractional stability condition, and the equilibrium points E_2 and E_3 are locally asymptotically stable. ∎

9. Global stability of the equilibria. In this section, we use the discretization technique to demonstrate the global stability of measles disease population extinction. We attempt to conceptualize the global stability of the system by generalizing it as a collection of difference equations given discrete time intervals over which different decisions and actions are implemented. Let $\kappa = \left[\frac{t}{x}\right] x$. The system is discretized as follows:

$$\begin{aligned} {}_0^C D_t^\vartheta S(t) &= S(\kappa) b^\vartheta \left(1 - \frac{S(\kappa)}{K}\right) - \frac{\beta^\vartheta S(\kappa) I(\kappa)}{N} - (\mu_1^\vartheta + \omega^\vartheta + \psi_1^\vartheta + \psi_2^\vartheta) S(\kappa), \\ {}_0^C D_t^\vartheta V(t) &= S(\kappa)(\psi_1^\vartheta + \psi_2^\vartheta) - V(\kappa)(\mu_1^\vartheta + \tau_1^\vartheta + \tau_2^\vartheta), \\ {}_0^C D_t^\vartheta I(t) &= \frac{\beta^\vartheta S(\kappa) I(\kappa)}{N} + \omega^\vartheta S(\kappa) + \tau_1^\vartheta V(\kappa) - (\gamma^\vartheta + \delta^\vartheta + \mu_1^\vartheta + \theta^\vartheta + \zeta^\vartheta) I(\kappa), \\ {}_0^C D_t^\vartheta R(t) &= (\gamma^\vartheta + \theta^\vartheta + \zeta^\vartheta \xi) I(\kappa) - \mu_1^\vartheta R(\kappa) + \tau_2^\vartheta V(\kappa), \end{aligned}$$

ETNA
Kent State University and
Johann Radon Institute (RICAM)

$$ {}_0^C D_t^\vartheta M(t) = \zeta^\vartheta I(\kappa) - \zeta^\vartheta \xi I(\kappa) - \mu_2^\vartheta M(\kappa). $$

Starting with $t \in [0, h)$ and $\frac{t}{h} \in [0, 1)$, we get

$$
\begin{aligned}
{}_0^C D_t^\vartheta S(t) &= S_0 b^\vartheta \left(1 - \frac{S_0}{K}\right) - \frac{\beta^\vartheta S_0 I_0}{N} - (\mu_1^\vartheta + \omega^\vartheta + \psi_1^\vartheta + \psi_2^\vartheta) S_0, \\
{}_0^C D_t^\vartheta V(t) &= S_0(\psi_1^\vartheta + \psi_2^\vartheta) - V_0(\mu_1^\vartheta + \tau_1^\vartheta + \tau_2^\vartheta), \\
{}_0^C D_t^\vartheta I(t) &= \frac{\beta^\vartheta S_0 I_0}{N} + \omega^\vartheta S(\kappa) + \tau_1^\vartheta V_0 - (\gamma^\vartheta + \delta^\vartheta + \mu_1^\vartheta + \theta^\vartheta + \zeta^\vartheta) I_0, \\
{}_0^C D_t^\vartheta R(t) &= (\gamma^\vartheta + \theta^\vartheta + \zeta^\vartheta \xi) I_0 - \mu_1^\vartheta R_0 + \tau_2^\vartheta V_0, \\
{}_0^C D_t^\vartheta M(t) &= \zeta^\vartheta I_0 - \zeta^\vartheta \xi I_0 - \mu_2^\vartheta M_0.
\end{aligned}
$$

The solution reduces to

$$
\begin{aligned}
S_1(t) &= S_0 + \frac{t^\vartheta}{\Gamma(\vartheta+1)} \left(S_0 b^\vartheta \left(1 - \frac{S_0}{K}\right) - \frac{\beta^\vartheta S_0 I_0}{N} - (\mu_1^\vartheta + \omega^\vartheta + \psi_1^\vartheta + \psi_2^\vartheta) S_0 \right), \\
V_1(t) &= V_0 + \frac{t^\vartheta}{\Gamma(\vartheta+1)} \left(S_0(\psi_1^\vartheta + \psi_2^\vartheta) - V_0(\mu_1^\vartheta + \tau_1^\vartheta + \tau_2^\vartheta) \right), \\
I_1(t) &= I_0 + \frac{t^\vartheta}{\Gamma(\vartheta+1)} \left(\frac{\beta^\vartheta S_0 I_0}{N} + \omega^\vartheta S_0 + \tau_1^\vartheta V_0 - (\gamma^\vartheta + \delta^\vartheta + \mu_1^\vartheta + \theta^\vartheta + \zeta^\vartheta) I_0 \right), \\
R_1(t) &= R_0 + \frac{t^\vartheta}{\Gamma(\alpha+1)} \left((\gamma^\vartheta + \theta^\vartheta + \zeta^\vartheta \xi) I_0 - \mu_1^\vartheta R_0 + \tau_2^\vartheta V_0 \right), \\
M_1(t) &= M_0 + \frac{t^\vartheta}{\Gamma(\vartheta+1)} \left(\zeta^\vartheta I_0 - \zeta^\vartheta \xi I_0 - \mu_2^\vartheta M_0 \right).
\end{aligned}
$$

For $t \in [h, 2h)$, $\frac{t}{h} \in [1, 2)$, we obtain

$$
\begin{aligned}
S_2(t) &= S_1 + \frac{(t-h)^\vartheta}{\Gamma(\vartheta+1)} \left(S_1 b^\vartheta \left(1 - \frac{S_1}{K}\right) - \frac{\beta^\vartheta S_1 I_1}{N} - (\mu_1^\vartheta + \omega^\vartheta + \psi_1^\vartheta + \psi_2^\vartheta) S_1 \right), \\
V_2(t) &= V_1 + \frac{(t-h)^\vartheta}{\Gamma(\vartheta+1)} \left(S_1(\psi_1^\vartheta + \psi_2^\vartheta) - V_1(\mu_1^\vartheta + \tau_1^\vartheta + \tau_2^\vartheta) \right), \\
I_2(t) &= I_1 + \frac{(t-h)^\vartheta}{\Gamma(\vartheta+1)} \left(\frac{\beta^\vartheta S_1 I_1}{N} + \omega^\vartheta S_1 + \tau_1^\vartheta V_1 - (\gamma^\vartheta + \delta^\vartheta + \mu_1^\vartheta + \theta^\vartheta + \zeta^\vartheta) I_1 \right), \\
R_2(t) &= R_1 + \frac{(t-h)^\vartheta}{\Gamma(\vartheta+1)} \left((\gamma^\vartheta + \theta^\vartheta + \zeta^\vartheta \xi) I_1 - \mu_1^\vartheta R_1 + \tau_2^\vartheta V_1 \right), \\
M_2(t) &= M_1 + \frac{(t-h)^\vartheta}{\Gamma(\vartheta+1)} \left(\zeta^\vartheta I_1 - \zeta^\vartheta \xi I_1 - \mu_2^\vartheta M_1 \right).
\end{aligned}
$$

In repeating the discretization process n times, we get

$$
\begin{aligned}
S_{n+1}(t) &= S_n + \frac{(t-nh)^\vartheta}{\Gamma(\vartheta+1)} \left(S_n b^\vartheta \left(1 - \frac{S_n}{k^\vartheta}\right) - \frac{\beta^\vartheta S_n I_n}{N} - (\mu_1^\vartheta + \omega^\vartheta + \psi_1^\vartheta + \psi_2^\vartheta) S_1 \right), \\
V_{n+1}(t) &= V_n + \frac{(t-nh)^\vartheta}{\Gamma(\vartheta+1)} \left(S_n(\psi_1^\vartheta + \psi_2^\vartheta) - V_n(\mu_1^\vartheta + \tau_1^\vartheta + \tau_2^\vartheta) \right)), \\
I_{n+1}(t) &= I_n + \frac{(t-nh)^\vartheta}{\Gamma(\vartheta+1)} \left(\frac{\beta^\vartheta S_n I_n}{N} + \omega^\vartheta S_n + \tau_1^\vartheta V_n - (\gamma^\vartheta + \delta^\vartheta + \mu_1^\vartheta + \theta^\vartheta + \zeta^\vartheta) I_n \right),
\end{aligned}
$$

ETNA
Kent State University and
Johann Radon Institute (RICAM)

$$R_{n+1}(t) = R_n + \frac{(t-nh)^{\vartheta}}{\Gamma(\vartheta+1)}\left(\gamma^{\vartheta} + \theta^{\vartheta} + \zeta^{\vartheta}\xi)I_n - \mu_1^{\vartheta}R_n + \tau_2^{\vartheta}V_n\right),$$
$$M_{n+1}(t) = M_n + \frac{(t-nh)^{\vartheta}}{\Gamma(\vartheta+1)}\left(\zeta^{\vartheta}I_n - -\zeta^{\vartheta}\xi I_n - \mu_2^{\vartheta}M_n\right).$$

Finally, for $t \in [nh, (n+1)h)$, where $t \to (n+1)h$ and $\vartheta \to 1$, we obtain

$$S_{n+1}(t) = S_n + \frac{h^{\vartheta}}{\Gamma(\vartheta+1)}\left(S_n b^{\vartheta}\left(1 - \frac{S_n}{K}\right) - \frac{\beta^{\vartheta}S_nI_n}{N} - (\mu_1^{\vartheta} + \omega^{\vartheta} + \psi_1^{\vartheta} + \psi_2^{\vartheta})S_n\right),$$
$$V_{n+1}(t) = V_n + \frac{h^{\vartheta}}{\Gamma(\vartheta+1)}\left(S_n(\psi_1^{\vartheta} + \psi_2^{\vartheta}) - V_n(\mu_1^{\vartheta} + \tau_1^{\vartheta} + \tau_2^{\vartheta})\right),$$
$$I_{n+1}(t) = I_n + \frac{h^{\vartheta}}{\Gamma(\vartheta+1)}\left(\frac{\beta^{\vartheta}S_nI_n}{N} + \omega^{\vartheta}S_n + \tau_1^{\vartheta}V_n - (\gamma^{\vartheta} + \delta^{\vartheta} + \mu_1^{\vartheta} + \theta^{\vartheta} + \zeta^{\vartheta})I_n\right),$$
$$R_{n+1}(t) = R_n + \frac{h^{\vartheta}}{\Gamma(\vartheta+1)}\left(\gamma^{\vartheta} + \theta^{\vartheta} + \zeta^{\vartheta}\xi)I_n - \mu_1^{\vartheta}R_n + \tau_2^{\vartheta}V_n\right),$$
$$M_{n+1}(t) = M_n + \frac{h^{\vartheta}}{\Gamma(\vartheta+1)}\left(\zeta^{\vartheta}I_n - \zeta^{\vartheta}\xi I_n - \mu_2^{\vartheta}M_n\right)).$$

LEMMA 9.1. *Assume that* $\{X(n)\}_{n=0}^{\infty} = \{(S(n), V(n), I(n), R(n), M(n))\}_{n=0}^{\infty}$ *is a positive solution of the system. Then the following conditions hold:*
(i) If

$$\begin{cases} S_n b^{\vartheta}\left(1 - \dfrac{S_n}{K}\right) - \dfrac{\beta^{\vartheta}S_nI_n}{N} - (\mu_1^{\vartheta} + \omega^{\vartheta} + \psi_1^{\vartheta} + \psi_2^{\vartheta})S_n > 0, \\ S_n(\psi_1^{\vartheta} + \psi_2^{\vartheta}) - V_n(\mu_1^{\vartheta} + \tau_1^{\vartheta} + \tau_2^{\vartheta}) > 0, \\ \dfrac{\beta^{\vartheta}S_nI_n}{N} + \omega^{\vartheta}S_n + \tau_1^{\vartheta}V_n - (\gamma^{\vartheta} + \delta^{\vartheta} + \mu_1^{\vartheta} + \theta^{\vartheta} + \zeta^{\vartheta})I_n > 0, \\ (\gamma^{\vartheta} + \theta^{\vartheta} + \zeta^{\vartheta}\xi)I_n - \mu_1^{\vartheta}R_n + \tau_2^{\vartheta}V_n > 0, \\ \zeta^{\vartheta}I_n - \zeta^{\vartheta}\xi I_n - \mu_2^{\vartheta}M_n > 0, \end{cases}$$

then the positive solution $\{X(n)\}_{n=0}^{\infty}$ *of the system is monotonically increasing.*
(ii) If

$$\begin{cases} S_n b^{\vartheta}\left(1 - \dfrac{S_n}{K}\right) - \dfrac{\beta^{\vartheta}S_nI_n}{N} - (\mu_1^{\vartheta} + \omega^{\vartheta} + \psi_1^{\vartheta} + \psi_2^{\vartheta})S_n < 0, \\ S_n(\psi_1^{\vartheta} + \psi_2^{\vartheta}) - V_n(\mu_1^{\vartheta} + \tau_1^{\vartheta} + \tau_2^{\vartheta}) < 0, \\ \dfrac{\beta^{\vartheta}S_nI_n}{N} + \omega^{\vartheta}S_n + \tau_1^{\vartheta}V_n - (\gamma^{\vartheta} + \delta^{\vartheta} + \mu_1^{\vartheta} + \theta^{\vartheta} + \zeta^{\vartheta})I_n < 0, \\ (\gamma^{\vartheta} + \theta^{\vartheta} + \zeta^{\vartheta}\xi)I_n - \mu_1^{\vartheta}R_n + \tau_2^{\vartheta}V_n < 0, \\ \zeta^{\vartheta}I_n - \zeta^{\vartheta}\xi I_n - \mu_2^{\vartheta}M_n < 0, \end{cases}$$

then the positive solution $\{X(n)\}_{n=0}^{\infty}$ *of the system is monotonically decreasing.*

Proof. The subsequent calculation arises from the analysis of the monotonic behavior of the solution in the system, as follows:

ETNA
Kent State University and
Johann Radon Institute (RICAM)

$$
\begin{aligned}
S_{n+1}(t) - S_n &= \frac{h^\vartheta}{\Gamma(\vartheta+1)}\left(S_n b^\vartheta\left(1-\frac{S_n}{K}\right) - \frac{\beta^\vartheta S_n I_n}{N}\right.\\
&\qquad\left. - (\mu_1^\vartheta + \omega^\vartheta + \psi_1^\vartheta + \psi_2^\vartheta)S_n\right),\\
V_{n+1}(t) - V_n &= \frac{h^\vartheta}{\Gamma(\vartheta+1)}\left(S_n(\psi_1^\vartheta+\psi_2^\vartheta) - V_n(\mu_1^\vartheta+\tau_1^\vartheta+\tau_2^\vartheta)\right)),\\
I_{n+1}(t) - I_n &= \frac{h^\vartheta}{\Gamma(\vartheta+1)}\left(\frac{\beta^\vartheta S_n I_n}{N} + \omega^\vartheta S_n + \tau_1^\vartheta V_n\right.\\
&\qquad\left. - (\gamma^\vartheta + \delta^\vartheta + \mu_1^\vartheta + \theta^\vartheta + \zeta^\vartheta)I_n\right),\\
R_{n+1}(t) - R_n &= \frac{h^\vartheta}{\Gamma(\vartheta+1)}\left((\gamma^\vartheta + \theta^\vartheta + \zeta^\vartheta\xi)I_n - \mu_1^\vartheta R_n + \tau_2^\vartheta V_n\right),\\
M_{n+1}(t) - M_n &= \frac{h^\vartheta}{\Gamma(\vartheta+1)}\left(\zeta^\vartheta I_n - \zeta^\vartheta\xi I_n - \mu_2^\vartheta M_n\right).
\end{aligned}
$$

Therefore, it becomes evident that under the conditions stated in (i), the system exhibits the following property:

$$S_{n+1} > S_n, \quad V_{n+1} > V_n, \quad I_{n+1} > I_n, \quad R_{n+1} > R_n, \quad \text{and} \quad M_{n+1} > M_n,$$

and, based on the conditions in (ii), we have

$$S_{n+1} < S_n, \quad V_{n+1} < V_n, \quad I_{n+1} < I_n, \quad R_{n+1} < R_n, \quad \text{and} \quad M_{n+1} < M_n, \qquad \square$$

THEOREM 9.2. *Let χ_1 be a coexisting equilibrium point of the system. Assume that the local stability conditions and those of Lemma 9.1 hold. If*

$$
\begin{aligned}
h_1 &< \left(\frac{2\left(S_n - \bar{S}_1\right)\Gamma(\vartheta+1)}{-\left(S_n b^\vartheta\left(1-\frac{S_n}{K}\right) + \frac{\beta^\vartheta S_n I_n}{N} - (\mu_1^\vartheta + \omega^\vartheta + \psi_1^\vartheta + \psi_2^\vartheta)S_n\right)}\right)^{\frac{1}{\vartheta}},\\
h_2 &< \left(\frac{2\left(V_n - \bar{V}_1\right)\Gamma(\vartheta+1)}{-\left(S_n(\psi_1^\vartheta+\psi_2^\vartheta) - (\mu_1^\vartheta+\tau_1^\vartheta+\tau_2^\vartheta)V_n\right)}\right)^{\frac{1}{\vartheta}},\\
h_3 &< \left(\frac{2\left(I_n - \bar{I}_1\right)\Gamma(\vartheta+1)}{-\left(\frac{\beta^\vartheta S_n I_n}{N} + \omega^\vartheta S_n + \tau_1^\vartheta V_n - (\gamma^\vartheta + \delta^\vartheta + \mu_1^\vartheta + \theta^\vartheta + \zeta^\vartheta)I_n\right)}\right)^{\frac{1}{\vartheta}},\\
h_4 &< \left(\frac{2\left(R_n - \bar{R}_1\right)\Gamma(\vartheta+1)}{-\left((\gamma^\vartheta + \theta^\vartheta + \zeta^\vartheta\xi)I_n - \mu_1^\vartheta R_n + \tau_2^\vartheta V_n\right)}\right)^{\frac{1}{\vartheta}},\\
h_5 &< \left(\frac{2\left(M_n - \bar{M}_1\right)\Gamma(\vartheta+1)}{-\left(\zeta^\vartheta I_n - \zeta^\vartheta\xi I_n - \mu_2^\vartheta M_n\right)}\right)^{\frac{1}{\vartheta}},
\end{aligned}
$$

where $S_n > \bar{S}_1, V_n > \bar{V}_1, I_n > \bar{I}_1, R_n > \bar{R}_1$, and $M_n > \bar{M}_1$, then the equilibrium point χ_1 is globally asymptotically stable.

ETNA
Kent State University and
Johann Radon Institute (RICAM)

Proof. Let us consider a Lyapunov function $L_y(n)$ defined by

$$L_y(n) = (X(n) - \chi_1)^2, \qquad n = 0, 1, 2, \ldots,$$

where $X(n) = (S(n), V(n), I(n), R(n), M(n))$ and $\chi_1 = \left(\bar{S}_1, \bar{V}_1, \bar{I}_1, \bar{R}_1, \bar{M}_1\right)$. Its change along the solutions of the system is

$$\begin{aligned}\Delta L_y(n) &= L_y(n+1) - L_y(n)\\ &= (X(n+1) - \chi_1)^2 - (X(n) - \chi_1)^2\\ &= (X(n+1) - X(n))\,(X(n+1) + X(n) - 2\chi_1)\,.\end{aligned}$$

From the first equation of the system (3.1), we have

$$\Delta L_{y_1}(n) = (L(n+1) - L(n))(L(n+1) + L(n)).$$

Using Lemma 9.1, it is evident that $L(n+1) < L(n)$. Hence, we only need to demonstrate that

$$L(n+1) + L(n) > 0,$$

which holds for

$$h_1 < \left(\frac{2\left(S_n - \bar{S}_1\right)\Gamma(\vartheta+1)}{-\left(S_n b^{\vartheta}\left(1 - \frac{S_n}{K}\right) + \frac{\beta^{\vartheta} S_n I_n}{N} - (\mu_1^{\vartheta} + \omega^{\vartheta} + \psi_1^{\vartheta} + \psi_2^{\vartheta})S_n\right)} \right)^{\frac{1}{\vartheta}}, \quad S_n > \bar{S}_1.$$

Thus, we obtain $\Delta L_{y_2}(n) < 0$. Similar to the previous computations, we can analyze

$$\Delta L_{y_2}(n) = (V(n+1) - V(n))(V(n+1) + V(n) - 2\bar{V}_1).$$

Using Lemma 9.1 (ii), it is obvious that $V(n+1) < V(n)$. Hence, we only need to demonstrate that

$$L_y(n+1) + L_y(n) > 0,$$

which holds for

$$h_2 < \left(\frac{2\left(V_n - \bar{V}_1\right)\Gamma(\vartheta+1)}{-\left(S_n(\psi_1^{\vartheta} + \psi_2^{\vartheta}) - (\mu_1^{\vartheta} + \tau_1^{\vartheta} + \tau_2^{\vartheta})V_n\right)} \right)^{\frac{1}{\vartheta}}, \quad V_n > \bar{V}_1.$$

Thus, we obtain $\Delta L_{y_3}(n) < 0$. Similar to the previous computations, we can analyze

$$\Delta Ly_3(n) = (I(n+1) - I(n))\left(I(n+1) + I(n) - 2\bar{I}_1\right).$$

From Lemma 9.1 (ii), we can show that $\Delta L_i(n) < 0$, for $i = 3, \ldots, 5$, if

$$h_3 < \left(\frac{2\left(I_n - \bar{I}_1\right)\Gamma(\vartheta+1)}{-\left(\frac{\beta^{\vartheta} S_n I_n}{N} + \omega^{\vartheta} S_n + \tau_1^{\vartheta} V_n - (\gamma^{\vartheta} + \delta^{\vartheta} + \mu_1^{\vartheta} + \theta^{\vartheta} + \zeta^{\vartheta})I_n\right)} \right)^{\frac{1}{\vartheta}}, \text{ for } I_n > \bar{I}_1,$$

$$h_4 < \left(\frac{2\left(R_n - \bar{R}_1\right)\Gamma(\vartheta+1)}{-\left((\gamma^{\vartheta} + \theta^{\vartheta} + \zeta^{\vartheta}\xi)I_n - \mu_1^{\vartheta} R_n + \tau_2^{\vartheta} V_n\right)} \right)^{\frac{1}{\vartheta}}, \qquad \text{for } R_n > \bar{R}_1,$$

$$h_5 < \left(\frac{2\left(R_n - \bar{R}_1\right)\Gamma(\vartheta+1)}{-\left(\zeta^{\vartheta} I_n - \zeta^{\vartheta}\xi I_n - \mu_2^{\vartheta} M_n\right)} \right)^{\frac{1}{\vartheta}}, \qquad \text{for } M_n > \bar{M}_1.$$

□

ETNA
Kent State University and
Johann Radon Institute (RICAM)

10. Numerical scheme for the provided measles model in the Caputo Fractional (CF) derivative sense. We employ the CF operator in order to analyze the behavior of the suggested fractional-order model. The Adams-type estimator-corrector approach [12, 13, 17, 18] is employed to provide a numerical simulation of the proposed nonlinear fractional-order system. Regarding the Caputo operator of order ϑ, the Cauchy-type ODE given below is considered:

$$ {}_0^C D_t^{\vartheta}\Phi(t) = f(t,\Phi(t)), \qquad \Phi^{(b)}(0) = \Phi_0^{(b)}, \qquad 0 < b \le n-1,\ 0 < t \le \tau, \tag{10.1}$$

where $b = 0, 1, \dots, n-1$, and $n = \lceil \vartheta \rceil$. Equation (10.1) can be transformed into the Volterra integral equation

$$ \Phi(t) = \sum_{b=0}^{n-1} \Phi_0^{(b)} \frac{t^b}{b!} + \frac{1}{\Gamma(\vartheta)} \int_0^t (t-s)^{\vartheta-1} f(s,\Phi(s))\, ds. \tag{10.2}$$

Taking into account the Adams–Bashforth–Moulton algorithm [12] and the proposed predictor–corrector scheme for the numerical solution of the model, we set

$$ h = \frac{\tau}{N}, \qquad t_z = zh, \qquad z = 0, 1, \dots, N \in \mathbb{Z}^+,$$

and denote $\Phi_z \approx \Phi(t_z)$.

Then the corresponding corrector formula [25] can be written as follows:

$$\begin{aligned}
S_{q+1} &= \sum_{z=0}^{q-1} S_0^{(z)} \frac{t_{q+1}^z}{z!} \\
&\quad + \frac{h^{\vartheta}}{\Gamma(\vartheta+2)} \sum_{z=0}^{q} p_{z,q+1} \Big[S_z b^{\vartheta} \Big(1 - \frac{S_z}{K}\Big) - \frac{\beta^{\vartheta} S_z I_z}{N} \\
&\qquad\qquad - (\mu_1^{\vartheta} + \omega^{\vartheta} + \psi_1^{\vartheta} + \psi_2^{\vartheta}) S_z \Big] \\
&\quad + \frac{h^{\vartheta}}{\Gamma(\vartheta+2)}\, p_{q+1,q+1} \Big[S_{q+1}^{PF} b^{\vartheta} \Big(1 - \frac{S_{q+1}^{PF}}{K}\Big) - \frac{\beta^{\vartheta} S_{q+1}^{PF} I_{q+1}^{PF}}{N} \\
&\qquad\qquad - (\mu_1^{\vartheta} + \omega^{\vartheta} + \psi_1^{\vartheta} + \psi_2^{\vartheta}) S_{q+1}^{PF} \Big].
\end{aligned}$$

$$\begin{aligned}
V_{q+1} &= \sum_{z=0}^{q-1} V_0^{(z)} \frac{t_{q+1}^z}{z!} \\
&\quad + \frac{h^{\vartheta}}{\Gamma(\vartheta+2)} \sum_{z=0}^{q} (p_{z,q+1}) \left(S_z(\psi_1^{\vartheta} + \psi_2^{\vartheta}) - \mu_1^{\vartheta} V_z - \left(\tau_1^{\vartheta} + \tau_2^{\vartheta}\right) V_z \right), \\
&\quad + \frac{h^{\vartheta}}{\Gamma(\vartheta+2)} \sum_{z=0}^{q} (p_{q+1,q+1}) \left(S_{q+1}^{PF}(\psi_1^{\vartheta} + \psi_2^{\vartheta}) - \mu_1^{\vartheta} V_{q+1}^{PF} - \left(\tau_1^{\vartheta} + \tau_2^{\vartheta}\right) V_{q+1}^{PF} \right),
\end{aligned}$$

$$\begin{aligned}
I_{q+1} &= \sum_{z=0}^{q-1} I_0^{(z)} \frac{t_{q+1}^z}{z!} \\
&\quad + \frac{h^{\vartheta}}{\Gamma(\vartheta+2)} \sum_{z=0}^{q} (p_{z,q+1}) - I_z \left(\gamma^{\vartheta} + \delta^{\vartheta} + \zeta^{\vartheta} + \theta^{\vartheta} + \mu_1^{\vartheta}\right) \\
&\quad + \frac{I_z \beta^{\vartheta} S_z}{N} + S_z \omega^{\vartheta} + \tau_1^{\vartheta} V_z
\end{aligned}$$

ETNA
Kent State University and
Johann Radon Institute (RICAM)

$$
\begin{aligned}
&+ \frac{h^{\vartheta}}{\Gamma(\vartheta+2)} \sum_{z=0}^{q} \left(p_{q+1,q+1}\right) \frac{I_{q+1}^{PF} \beta^{\vartheta} S_{q+1}^{PF}}{N} + S_{q+1}^{PF} \omega^{\vartheta} \\
&+ \tau_1^{\vartheta} V_{q+1}^{PF} - I_{q+1}^{PF} \left(\gamma^{\vartheta} + \delta^{\vartheta} + \zeta^{\vartheta} + \theta^{\vartheta} + \mu_1^{\vartheta}\right), \\
R_{q+1} = &\sum_{z=0}^{q-1} R_0^{(z)} \frac{t_{q+1}^{z}}{z!} \\
&+ \frac{h^{\vartheta}}{\Gamma(\vartheta+2)} \sum_{z=0}^{q} \left(p_{z,q+1}\right) I_z(\gamma^{\vartheta} + \theta^{\vartheta}) + I_z \zeta^{\vartheta} - \mu_1^{\vartheta} R_z + \tau_2^{\vartheta} V_z \\
&+ \frac{h^{\vartheta}}{\Gamma(\vartheta+2)} \sum_{z=0}^{q} \left(p_{q+1,q+1}\right) I_{q+1}^{PF}(\gamma^{\vartheta} + \theta^{\vartheta}) + I_{q+1}^{PF} \zeta^{\vartheta} - \mu_1^{\vartheta} R_{q+1}^{PF} + \tau_2^{\vartheta} V_{q+1}^{PF}, \\
M_{q+1} = &\sum_{z=0}^{q-1} M_0^{(z)} \frac{t_{q+1}^{z}}{z!} \\
&+ \frac{h^{\vartheta}}{\Gamma(\vartheta+2)} \sum_{z=0}^{q} \left(p_{z,q+1}\right) I_z \zeta^{\vartheta} - I_z \zeta^{\vartheta} - \mu_2^{\vartheta} M_z \\
&+ \frac{h^{\vartheta}}{\Gamma(\vartheta+2)} \sum_{z=0}^{q} \left(p_{q+1,q+1}\right) I_{q+1}^{PF} \zeta^{\vartheta} - I_{q+1}^{PF} \zeta^{\vartheta} - \mu_2^{\vartheta} M_{q+1}^{PF},
\end{aligned}
$$

where

$$
p_{z,q+1} = \begin{cases} q^{\vartheta+1} - (q-\vartheta)(q+1)^{\vartheta}, & \text{if } z = 0, \\ (q-z+2)^{\vartheta+1} + (q-z)^{\vartheta+1} - 2(q-z+1)^{\vartheta+1}, & \text{if } 1 \le z \le q, \\ 1, & \text{if } z = q+z. \end{cases}
$$

The predictor formula for the next step, Φ_{q+1}^{PF}, is given by

$$
\begin{aligned}
S_{q+1}^{PF} = &\sum_{z=0}^{q-1} S_0^{(z)} \frac{t_{q+1}^{z}}{z!} + \frac{h^{\vartheta}}{\Gamma(\vartheta+1)} \sum_{z=0}^{q} \Bigg(\left(j_{z,q+1}\right) \; S_z b^{\vartheta} \left(1 - \frac{S_z}{K}\right) + \frac{\beta^{\vartheta} S_z I_z}{N} \\
&\qquad - (\mu_1^{\vartheta} + \omega^{\vartheta} + \psi_1^{\vartheta} + \psi_2^{\vartheta}) S_z, \Bigg) \\
V_{q+1}^{PF} = &\sum_{z=0}^{q-1} I_0^{(z)} \frac{t_{q+1}^{z}}{z!} \\
&+ \frac{h^{\vartheta}}{\Gamma(\vartheta+1)} \sum_{z=0}^{q} \left(j_{z,q+1}\right) \left(S_z(\psi_1^{\vartheta} + \psi_2^{\vartheta}) - \mu_1^{\vartheta} V_z - \left(\tau_1^{\vartheta} + \tau_2^{\vartheta}\right) V_z\right), \\
I_{q+1}^{PF} = &\sum_{z=0}^{q-1} I_0^{(z)} \frac{t_{q+1}^{z}}{z!} \\
&+ \frac{h^{\vartheta}}{\Gamma(\vartheta+1)} \sum_{z=0}^{q} \Bigg(\left(j_{z,q+1}\right) \left(\gamma^{\vartheta} + \delta^{\vartheta} + \zeta^{\vartheta} + \theta^{\vartheta} + \mu_1^{\vartheta}\right) I_z \\
&\qquad + \frac{I_z \beta^{\vartheta} S_z}{N} + S_z \omega^{\vartheta} + \tau_1^{\vartheta} V_z, \Bigg)
\end{aligned}
$$

ETNA
Kent State University and
Johann Radon Institute (RICAM)

$$R_{q+1}^{PF} = \sum_{z=0}^{q-1} R_0^{(z)} \frac{t_{q+1}^z}{z!} + \frac{h^\vartheta}{\Gamma(\vartheta+1)} \sum_{z=0}^{q} \Big((j_{z,q+1})\, I_z(\gamma^\vartheta + \theta^\vartheta) + I_z\zeta^\vartheta - \mu_1^\vartheta R_z + \tau_2^\vartheta V_z, \Big)$$

$$M_{q+1}^{PF} = \sum_{z=0}^{q-1} M_0^{(z)} \frac{t_{q+1}^z}{z!} + \frac{h^\vartheta}{\Gamma(\vartheta+1)} \sum_{z=0}^{q} (j_{z,q+1})\, I_z\zeta^\vartheta - I_z\zeta^\vartheta - \mu_2^\vartheta M_z,$$

where

$$j_{z,q+1} = (q+1-z)^\vartheta - (q-z)^\vartheta.$$

11. Numerical simulations and discussion. Numerical simulations of the proposed fractional-order model are performed using the Adams–Bashforth–Moulton predictor-corrector algorithm [17]. The initial conditions are set as

$$(S_0, V_0, I_0, R_0, M_0) = (67{,}735{,}000, 100{,}568, 11, 10, 1),$$

and the parameter values are adopted from Table 12.1. The simulations are conducted to investigate how the system dynamics responds to variations in the fractional-order parameter ϑ and other key epidemiological parameters.

Figure 11.1 displays the time evolution of the susceptible population for different ϑ-values. The number of susceptible individuals declines until approximately day 20, after which it stabilizes. Smaller values of ϑ increase memory effects, slowing the stabilization process. Similarly, Figure 11.2 shows that the vaccinated population initially rises, then slightly decreases before stabilizing. The fractional-order memory delays the equilibrium when $\vartheta < 1$.

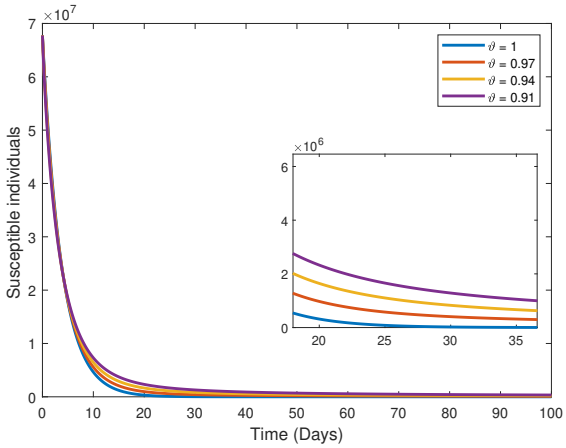

FIG. 11.1. *Change of susceptible individuals over time for different fractional-order derivative values ϑ.*

Figure 11.3 illustrates the infected population dynamics. The infection peaks around day 15 and subsequently declines toward equilibrium. Fractional-order effects reduce the peak magnitude and prolong the convergence to the steady state. The recovered population (Figure 11.4) reaches the equilibrium faster when $\vartheta = 1$, while the Reye's syndrome subpopulation (Figure 11.5) stabilizes more quickly at $\vartheta = 1$, confirming that the fractional-order dynamics delays the stabilization across the subpopulations.

ETNA
Kent State University and
Johann Radon Institute (RICAM)

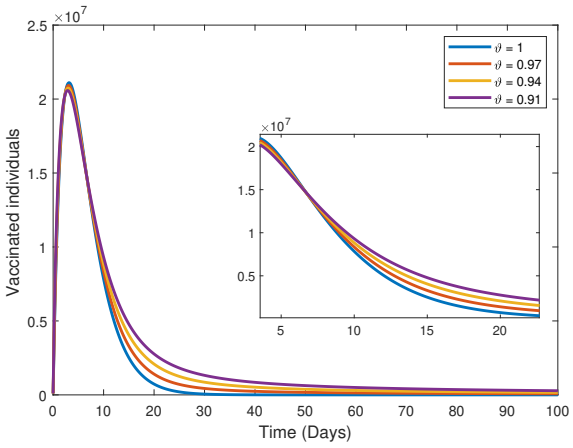

FIG. 11.2. *Change of infected individuals over time for different fractional-order derivative values ϑ .*

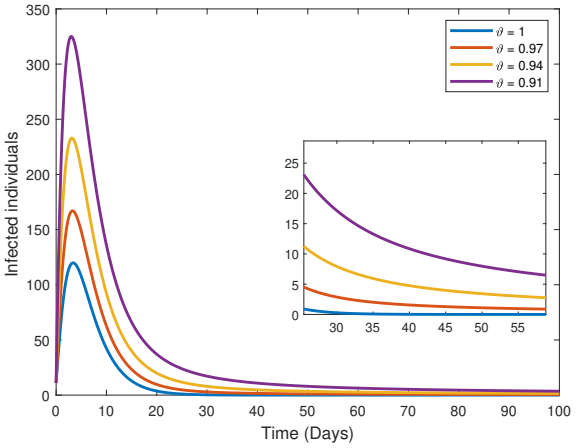

FIG. 11.3. *Change of infected individuals over time for different fractional-order derivative values ϑ.*

The influence of the transmission rate β is presented in Figure 11.6. Higher β-values accelerate the decline of susceptible individuals and increase the infection prevalence initially, before vaccination and recovery stabilize the system, which is consistent with the biological behavior of measles.

Figure 11.7 examine the vaccination parameters ψ_1 (first-dose rate) and ω (hesitancy). Increasing ψ_1 accelerates the susceptibility decline and improves coverage, whereas a higher ω slows the vaccination uptake, raising the infection risk.

The effects of aspirin administration are illustrated in Figure 11.8, represented by ζ and ξ. Increasing ζ reduces the infected and recovered populations but raises the incidence of Reye's syndrome, reflecting known pediatric risks. Conversely, increasing ξ promotes the recovery and mitigates the severity of Reye's syndrome.

Finally, Figure 11.9 shows that higher recovery rates γ lead to a faster decline in the infections and an increase in the recovered individuals, in agreement with expected biological outcomes.

ETNA
Kent State University and
Johann Radon Institute (RICAM)

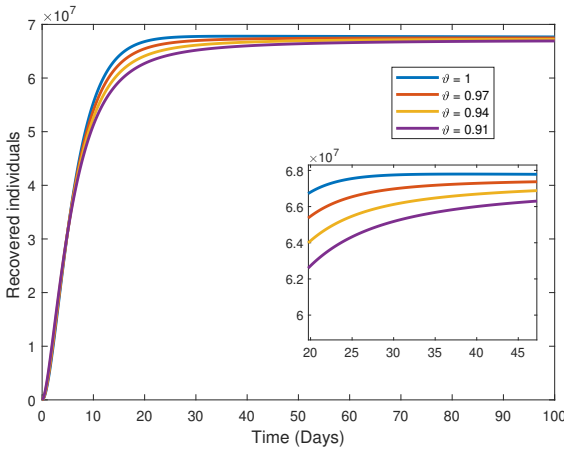

FIG. 11.4. *Change of recovered individuals over time for different fractional-order derivative values ϑ.*

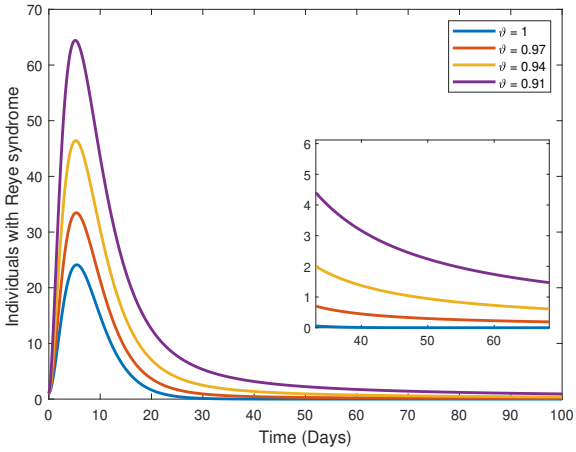

FIG. 11.5. *Time evolution of individuals with Reye's syndrome for different fractional-order values ϑ.*

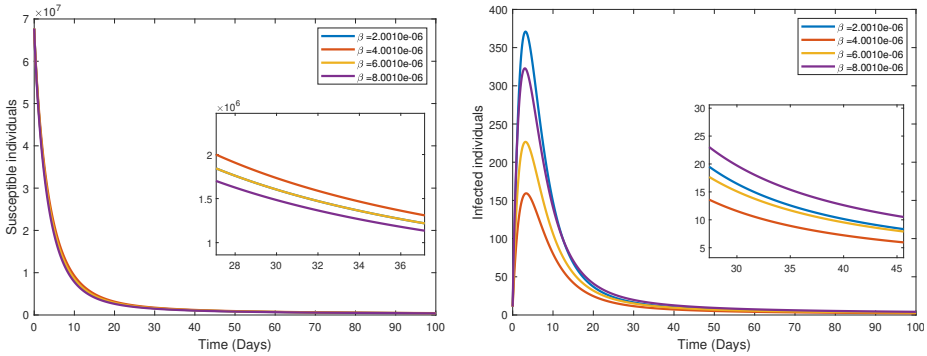

FIG. 11.6. *Dynamics of susceptible and infected individuals for different transmission rates β at $\vartheta = 0.94$.*

ETNA
Kent State University and
Johann Radon Institute (RICAM)

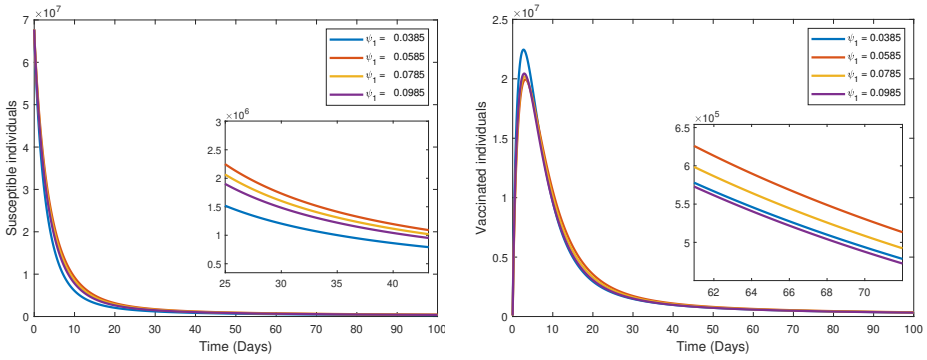

FIG. 11.7. *Dynamics of susceptible and vaccinated individuals for different vaccination rates ψ_1 at $\vartheta = 0.94$.*

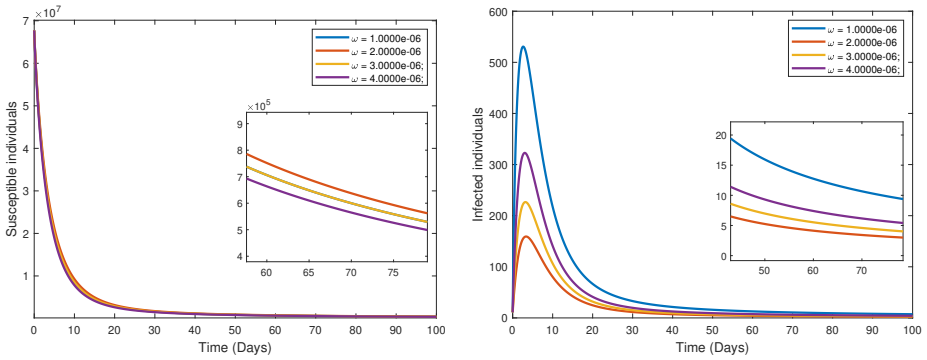

FIG. 11.8. *Dynamics of susceptible and infected individuals for different values of the vaccination hesitancy rate ω at $\vartheta = 0.94$.*

Overall, the numerical simulations demonstrate that fractional-order dynamics significantly influence the timing and magnitude of epidemic peaks and equilibrium states, while key epidemiological and behavioral parameters critically modulate the disease spread and the complication rates.

Figure 11.12 presents the sensitivity analysis of the endemic infected population with respect to the fractional-order parameter ϑ. The results demonstrate that the fractional-order parameter has a substantial influence on the disease transmission dynamics. Specifically, increasing ϑ toward 1 causes the system to gradually converge to the classical integer-order behavior, while smaller values of ϑ introduce stronger memory effects, leading to noticeable changes in the infected population level. These findings highlight the importance of incorporating fractional-order dynamics in accurately describing the spread and persistence of the measles infection.

The sensitivity analysis shown in Figure 11.13 indicates that the transmission rate β has the highest positive impact on the basic reproduction number R_0, while recovery, mortality, and vaccination-related parameters reduce the epidemic threshold. This suggests that controlling the transmission rate is the most effective strategy for disease mitigation.

Figure 11.14 illustrates the effect of the fractional-order parameter ϑ on the basic reproduction number R_0. It is observed that as ϑ increases, the value of R_0 decreases, indicating that memory effects play a stabilizing role in the epidemic dynamics and reduce disease persistence.

ETNA
Kent State University and
Johann Radon Institute (RICAM)

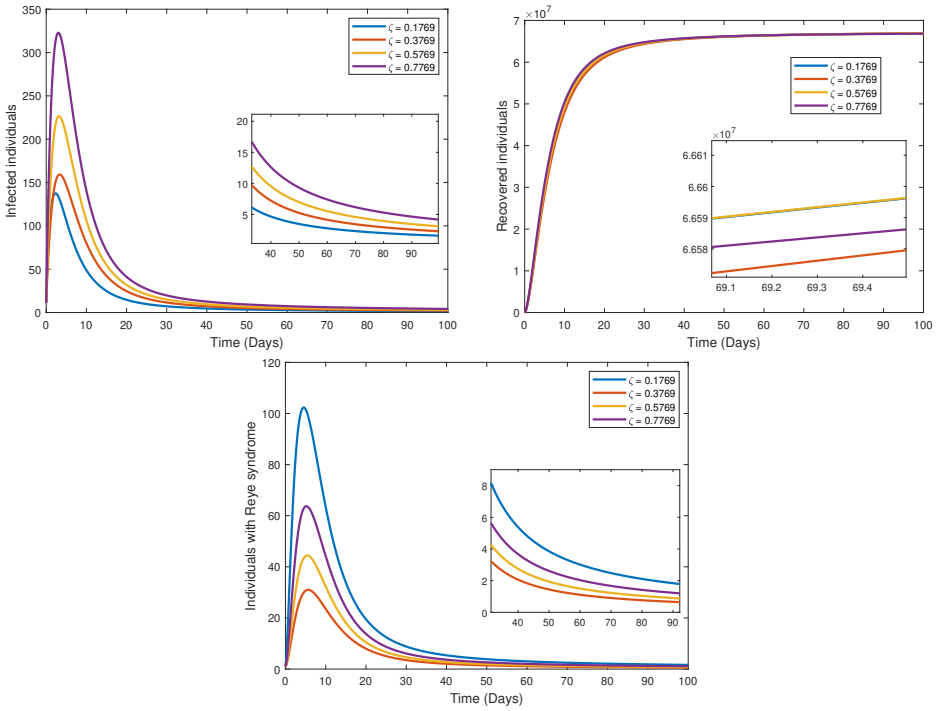

FIG. 11.9. *Effects of the aspirin usage rate ζ on recovered individuals and individuals with Reye's syndrome at $\vartheta = 0.94$.*

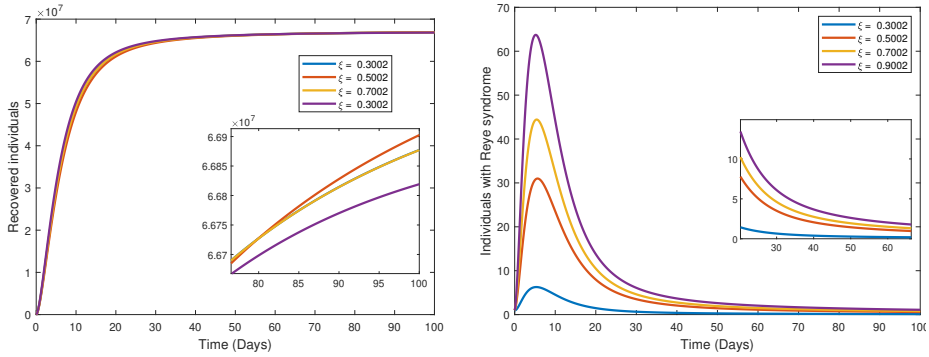

FIG. 11.10. *Effects of the recovery-through-aspirin rate ξ on recovered individuals and individuals with Reye's syndrome at $\vartheta = 0.94$.*

12. Parameter estimation. Parameter estimation is applied to obtain a curve closest fitting the real data such that the most appropriate parameter values are obtained with this method. Quite often, parameter values found in the literature are used in applications of the mathematical models, but their accurate estimation is very important in order to run a more realistic mathematical model, to increase the reliability of the considered model for the future prediction of the disease, and to allow a better understanding of the transmission dynamics of the epidemic.

ETNA
Kent State University and
Johann Radon Institute (RICAM)

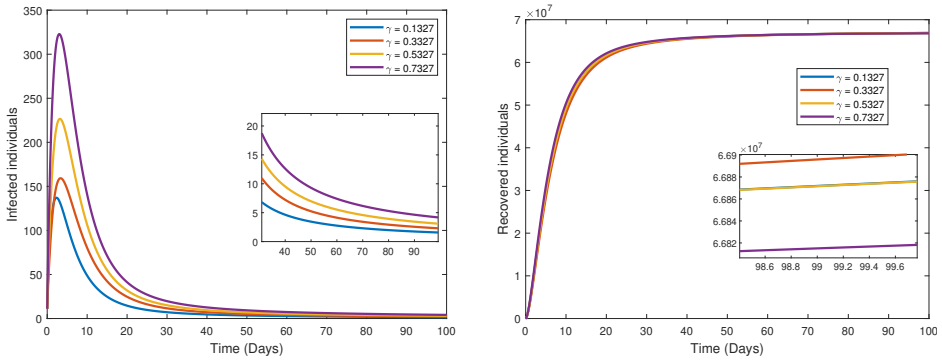

FIG. 11.11. *Dynamics of infected and recovered individuals for different recovery rates γ at $\vartheta = 0.94$.*

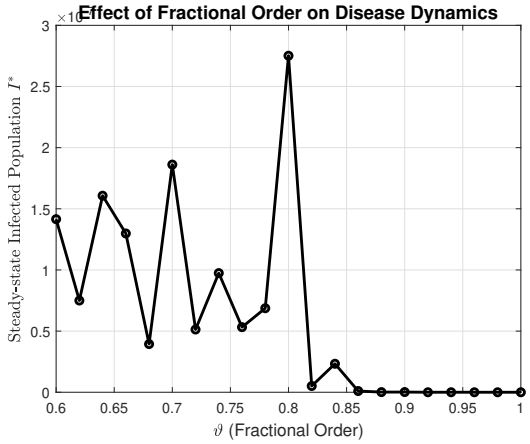

FIG. 11.12. *Sensitivity analysis of the endemic infected population with respect to the fractional-order parameter ϑ.*

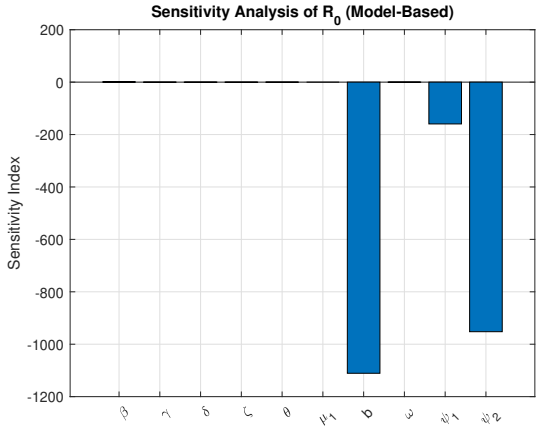

FIG. 11.13. *Sensitivity indices of the basic reproduction number R_0 with respect to model parameters.*

ETNA
Kent State University and
Johann Radon Institute (RICAM)

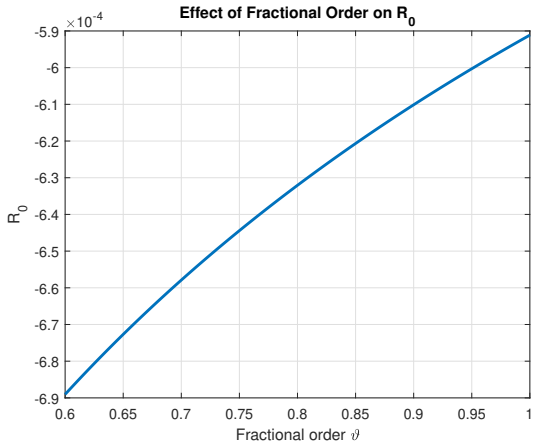

FIG. 11.14. *Effect of the fractional-order parameter ϑ on the basic reproduction number R_0.*

The model parameters are estimated in order to obtain the best-fitting curve to the observed measles incidence data. The estimation is performed using a nonlinear least-squares optimization framework, where the objective function is defined as the sum of the squared differences between the numerical solutions of the fractional-order system and the reported epidemiological data. The fractional-order system is solved numerically for each candidate parameter set, and the optimal parameters are obtained by minimizing this error criterion. In addition, the initial population values are determined based on demographic data, and consistency conditions are imposed to ensure biological feasibility. The results indicate that the fractional-order model provides a significantly improved fit to the real data, highlighting the importance of memory and hereditary effects in describing the transmission dynamics of measles.

There are 16 different parameter values in the measles model. We fit 16 of these parameter values using actual measles incidence data from the United Kingdom (WHO), calculated using the average UK life expectancy (81.4), μ_1 (natural mortality rate) (3.36575679e-5) (WHO), and the total population of the United Kingdom $(67, 835, 590)$. We covered 21 months of data cases from 2019 to 2023. If the initial conditions are the total UK population and the infected individuals, then $I(0) = 11$ and because $N(0) = S(0) + V(0) + I(0) + R(0) + M(0)$, $R(0) = 10$, and $M(0) = 1$, the remaining other population values are calculated as $S(0) = 67, 735, 000$ and $V(0) = 100, 568$.

Actual cases of measles are displayed as red-filled circles in Figure 12.1. Values that best fit the actual data are displayed with a blue line. The parameter values used in the model are given in Table 12.1, together with the best-fit values obtained using the Least-Squares Curve Fitting Technique (LSCFT).

13. Bifurcation analysis. To know the qualitative behavior of the solution of the given n-dimensional dynamical system

$$\frac{dx}{dt} = f(x, \mu), \qquad x \in \mathbb{R}^m, \tag{13.1}$$

near the non-hyperbolic equilibrium points as the vector field f passes through a point in the bifurcation set or as the parameter μ varies through a bifurcation value μ_0, we use the following criteria:

ETNA
Kent State University and
Johann Radon Institute (RICAM)

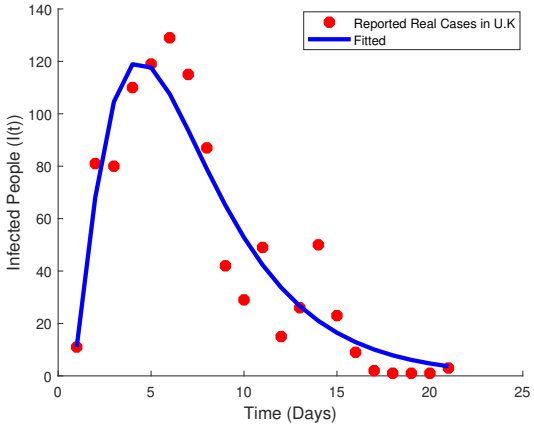

FIG. 12.1. *Real cases of measles in the U.K. from 2019–2023 and the best-fit curve from the proposed model.*

THEOREM 13.1 (Sotomayor's theorem). *Suppose that* $f(x_0, \mu_0) = 0$ *and that the* $n \times n$ *matrix* $A = Df(x_0, \mu_0)$ *has a simple eigenvalue* $\lambda = 0$ *with eigenvector* v *and that* A^T *has an eigenvector* w *corresponding to the eigenvalue* $\lambda = 0$*. Furthermore, suppose that* A *has* k *eigenvalues with negative real part and* $(n - k - 1)$ *eigenvalues with positive real part.*

1. *If* $w^T f_\mu(x_0, \mu_0) \neq 0, w^T[D^2 f(x_0, \mu_0)(v, v)] \neq 0$*, then the system* (13.1) *experiences a saddle-node bifurcation at the equilibrium point* x_0 *as the parameter* μ *passes through the bifurcation value* $\mu = \mu_0$*.*
2. *If* $w^T f_\mu(x_0, \mu_0) = 0, w^T[Df(x_0, \mu_0)v] \neq 0$*, and* $w^T[D^2 f(x_0, \mu_0)(v, v)] \neq 0$*, then the system* (13.1) *experiences a trans-critical bifurcation at the equilibrium point* x_0 *as the parameter* μ *varies through the bifurcation value* $\mu = \mu_0$*.*
3. *If* $w^T f_\mu(x_0, \mu_0) = 0, w^T[Df(x_0, \mu_0)v] \neq 0$*,* $w^T[D^2 f(x_0, \mu_0)(v, v)] = 0$*, and* $w^T[D^3 f(x_0, \mu_0)(v, v, v)] \neq 0$*, then the system* (13.1) *experiences a pitchfork bifurcation at the equilibrium point* x_0 *as the parameter* μ *varies through the bifurcation value* $\mu = \mu_0$*.*

Let the eigenvalue of $J(E_0)\big|_{\beta^*}$ be zero, and let the corresponding equilibrium system be given by:

$$
\begin{aligned}
&{}_0^C D_t^\vartheta S(t) = b^\vartheta S\left(1 - \frac{S}{K}\right) - S\left(\mu_1^\vartheta + \omega^\vartheta\right) - \frac{I\beta^\vartheta S}{N} - S(\psi_1^\vartheta + \psi_2^\vartheta) = f_1,\\
&{}_0^C D_t^\vartheta V(t) = S(\psi_1^\vartheta + \psi_2^\vartheta) - \left(\mu_1^\vartheta + \tau_1^\vartheta + \tau_2^\vartheta\right) V = f_2,\\
&{}_0^C D_t^\vartheta I(t) = -I\left(\gamma^\vartheta + \delta^\vartheta + \zeta^\vartheta + \theta^\vartheta + \mu_1^\vartheta\right) + \frac{I\beta^\vartheta S}{N} + S\omega^\vartheta + \tau_1^\vartheta V = f_3,\\
&{}_0^C D_t^\vartheta R(t) = I(\gamma^\vartheta + \theta^\vartheta) + I\zeta^\vartheta\xi - \mu_1^\vartheta R + \tau_2^\vartheta V = f_4,\\
&{}_0^C D_t^\vartheta M(t) = I\zeta^\vartheta(1 - \xi) - \mu_2^\vartheta M = f_5.
\end{aligned}
$$

Let

$$
\begin{aligned}
&x_0 = E_0(S, V, I, R, M) = (0, 0, 0, 0, 0),\\
&R_0 = \frac{\beta K(b - \mu_1 - \omega - \psi_1 - \psi_2)}{bN(\gamma + \delta + \zeta + \theta + \mu_1)} = 1,\\
&\mu_0 = \omega^* = \frac{\beta Kb - \beta K\mu_1 - \beta K\psi_1 - \beta K\psi_2 - bN(\gamma + \delta + \zeta + \theta + \mu_1)}{\beta K}.
\end{aligned}
$$

ETNA
Kent State University and
Johann Radon Institute (RICAM)

TABLE 12.1
The biological meanings of the parameters and their numerical values.

Par.	Description	Parameter est. values	Reference	Unit
β	transmission rate	2.0010e-06	fitted	1/year
ω	the rate of individuals with prejudice against vaccination	1.0000e-06	fitted	1/year
τ_1	the rate of people vaccinated against measles	1.1639e-06	fitted	1/year
τ_2	the rate of people vaccinated and cured of measles	0.3691	fitted	1/year
ψ_1	the rate of people who received the first dose of measles vaccine	0.0385	fitted	1/year
ψ_2	the rate of people who received the second dose of measles vaccine	0.2299	fitted	1/year
μ_1	the natural death rate of humans in the district	0.0000336575679	fitted	1/year
μ_2	death rate from Reye's syndrome	0.5224	fitted	1/year
θ	the rate of those taking vitamin A supplements	0.0943	fitted	1/year
b	logistic growth rate of susceptible individuals	2.4143e-04	fitted	1/year
ζ	the rate of people using aspirin during measles treatment	0.1769	fitted	1/year
ξ	the rate of those who were infected and recovered and became immune by using aspirin	0.3002	fitted	1/year
γ	the recovery rate of infected individuals	0.1327	fitted	1/year
δ	the death rate due to measles infection	0.0943	fitted	1/year
K	carrying capacity of the population	0.1325	fitted	1/year

Then,

$$Df(x,\mu) = \begin{bmatrix} a_{11} & 0 & a_{13} & 0 & 0 \\ \psi_1+\psi_2 & -\mu_1-\tau_1-\tau_2 & 0 & 0 & 0 \\ a_{31} & \tau_1 & a_{33} & 0 & 0 \\ 0 & \tau_2 & \gamma+\theta+\zeta\xi & -\mu_1 & 0 \\ 0 & 0 & \zeta-\zeta\xi & 0 & -\mu_2 \end{bmatrix},$$

where

$$\begin{aligned} a_{11} &= b\left(1-\frac{2S}{K}\right)-(\mu_1+\omega^*+\psi_1+\psi_2)-\frac{I\beta}{N}, \\ a_{13} &= -\frac{S\beta}{N}, \\ a_{31} &= \omega^*+\frac{I\beta}{N}, \\ a_{33} &= -(\zeta+\delta+\mu_1+\gamma+\theta)+\frac{S\beta}{N}, \end{aligned}$$

ETNA
Kent State University and
Johann Radon Institute (RICAM)

$$
\begin{aligned}
&Df(x_0,\mu_0)\\
&= \begin{bmatrix}
b-\mu_1-\omega^*-\psi_1-\psi_2 & 0 & 0 & 0 & 0\\
\psi_1+\psi_2 & -\mu_1-\tau_1-\tau_2 & 0 & 0 & 0\\
\omega^* & \tau_1 & -(\zeta+\delta+\mu_1+\gamma+\theta) & 0 & 0\\
0 & \tau_2 & \gamma+\theta+\zeta\xi & -\mu_1 & 0\\
0 & 0 & \zeta-\zeta\xi & 0 & -\mu_2
\end{bmatrix}\\
&= A,
\end{aligned}
$$

$$
\begin{aligned}
&D^2f(x_0,\mu_0)\\
&= \begin{bmatrix}
\frac{-2b^{\vartheta}}{K} & 0 & \frac{-\beta}{N} & 0 & 0 & 0 & 0 & 0 & 0 & \frac{-\beta}{N} & 0 & 0 & 0 & 0 & 0 & 0 & 0 & 0 & 0 & 0 & 0 & 0 & 0\\
0 & 0 & 0 & 0 & 0 & 0 & 0 & 0 & 0 & 0 & 0 & 0 & 0 & 0 & 0 & 0 & 0 & 0 & 0 & 0 & 0 & 0 & 0\\
0 & 0 & \frac{\beta}{N} & 0 & 0 & 0 & 0 & 0 & 0 & \frac{\beta}{N} & 0 & 0 & 0 & 0 & 0 & 0 & 0 & 0 & 0 & 0 & 0 & 0 & 0\\
0 & 0 & 0 & 0 & 0 & 0 & 0 & 0 & 0 & 0 & 0 & 0 & 0 & 0 & 0 & 0 & 0 & 0 & 0 & 0 & 0 & 0 & 0\\
0 & 0 & 0 & 0 & 0 & 0 & 0 & 0 & 0 & 0 & 0 & 0 & 0 & 0 & 0 & 0 & 0 & 0 & 0 & 0 & 0 & 0 & 0
\end{bmatrix}.
\end{aligned}
$$

We set $Av = 0$, where $v = (v_1, v_2, v_3, v_4, v_5)^T$ and $0 = (0,0,0,0,0)^T$:

$$
\begin{bmatrix}
b-\mu_1-\omega^*-\psi_1-\psi_2 & 0 & 0 & 0 & 0\\
\psi_1+\psi_2 & -\mu_1-\tau_1-\tau_2 & 0 & 0 & 0\\
\omega^* & \tau_1 & -(\zeta+\delta+\mu_1+\gamma+\theta) & 0 & 0\\
0 & \tau_2 & \gamma+\theta+\zeta\xi & -\mu_1 & 0\\
0 & 0 & \zeta-\zeta\xi & 0 & -\mu_2
\end{bmatrix}
\begin{bmatrix} v_1\\ v_2\\ v_3\\ v_4\\ v_5 \end{bmatrix}
= \begin{bmatrix} 0\\ 0\\ 0\\ 0\\ 0 \end{bmatrix},
$$

yielding

$$
\begin{aligned}
(b-\mu_1-\omega^*-\psi_1-\psi_2)v_1 &= 0 \qquad \text{(a)},\\
(\psi_1+\psi_2)v_1-(\mu_1+\tau_1+\tau_2)v_2 &= 0 \qquad \text{(b)},\\
\omega^*v_1+\tau_1v_2-(\zeta+\delta+\mu_1+\gamma+\theta)v_3 &= 0 \qquad \text{(c)},\\
\tau_2v_2+(\gamma+\theta+\zeta\xi)v_3-\mu_1v_4 &= 0 \qquad \text{(d)},\\
(\zeta-\zeta\xi)v_3-\mu_2v_5 &= 0 \qquad \text{(e)}.
\end{aligned}
$$

From (b), we have $v_2 = \frac{(\psi_1+\psi_2)v_1}{\mu_1+\tau_1+\tau_2}$. Substitution of v_3 in (c) provides $v_3 = \frac{\tau_1v_2+\omega^*v_1}{\zeta+\delta+\mu_1+\gamma+\theta}$. From (d) and (e), $v_4 = \frac{\tau_2v_2+(\gamma+\theta+\zeta\xi)v_3}{\mu_1}$, $v_5 = \frac{(\zeta-\zeta\xi)v_3}{\mu_2}$.

Let $v_1 = 1$. Thus,

$$
\begin{aligned}
v = \Bigg[1, &\frac{\psi_1+\psi_2}{\mu_1+\tau_1+\tau_2}, \frac{\tau_1v_1(\psi_1+\psi_2)+\omega^*v_1(\zeta+\delta+\mu_1+\gamma+\theta)}{(\mu_1+\tau_1+\tau_2)(\zeta+\delta+\mu_1+\gamma+\theta)},\\
&\frac{\tau_1v_1(\psi_1+\psi_2)+\omega^*v_1(\mu_1+\tau_1+\tau_2)}{(\mu_1+\tau_1+\tau_2)(\zeta+\delta+\mu_1+\gamma+\theta)},\\
&\frac{\tau_1v_1(\psi_1+\psi_2)+\omega^*v_1(\mu_1+\tau_1+\tau_2)(\zeta-\zeta\xi)}{(\mu_1+\tau_1+\tau_2)\mu_2(\zeta+\delta+\mu_1+\gamma+\theta)}\Bigg]^T,
\end{aligned}
$$

$$
\begin{aligned}
&(v,v)\\
&= \left(\begin{bmatrix}
1\\
\frac{\psi_1+\psi_2}{\mu_1+\tau_1+\tau_2}\\
\frac{\tau_1v_1(\psi_1+\psi_2)+\omega^*v_1(\zeta+\delta+\mu_1+\gamma+\theta)}{(\mu_1+\tau_1+\tau_2)(\zeta+\delta+\mu_1+\gamma+\theta)}\\
\frac{\tau_1v_1(\psi_1+\psi_2)+\omega^*v_1(\mu_1+\tau_1+\tau_2)}{(\mu_1+\tau_1+\tau_2)(\zeta+\delta+\mu_1+\gamma+\theta)}\\
\frac{\tau_1v_1(\psi_1+\psi_2)+\omega^*v_1(\mu_1+\tau_1+\tau_2)(\zeta-\zeta\xi)}{(\mu_1+\tau_1+\tau_2)\mu_2(\zeta+\delta+\mu_1+\gamma+\theta)})
\end{bmatrix}, \begin{bmatrix}
1\\
\frac{\psi_1+\psi_2}{\mu_1+\tau_1+\tau_2}\\
\frac{\tau_1v_1(\psi_1+\psi_2)+\omega^*v_1(\zeta+\delta+\mu_1+\gamma+\theta)}{(\mu_1+\tau_1+\tau_2)(\zeta+\delta+\mu_1+\gamma+\theta)}\\
\frac{\tau_1v_1(\psi_1+\psi_2)+\omega^*v_1(\mu_1+\tau_1+\tau_2)}{(\mu_1+\tau_1+\tau_2)(\zeta+\delta+\mu_1+\gamma+\theta)}\\
\frac{\tau_1v_1(\psi_1+\psi_2)+\omega^*v_1(\mu_1+\tau_1+\tau_2)(\zeta-\zeta\xi)}{(\mu_1+\tau_1+\tau_2)\mu_2(\zeta+\delta+\mu_1+\gamma+\theta)}
\end{bmatrix}\right)
\end{aligned}
$$

ETNA
Kent State University and
Johann Radon Institute (RICAM)

$$= \begin{bmatrix} a_1 \\ a_2 \\ . \\ . \\ . \\ a_{25} \end{bmatrix}.$$

The formulas for a_1–a_{25} are as follows:

$$a_1 = 1,$$
$$a_2 = \frac{\psi_1 + \psi_2}{\mu_1 + \tau_1 + \tau_2},$$
$$a_3 = \frac{\tau_1 v_1(\psi_1 + \psi_2) + \omega^* v_1(\zeta + \delta + \mu_1 + \gamma + \theta)}{(\mu_1 + \tau_1 + \tau_2)(\zeta + \delta + \mu_1 + \gamma + \theta)},$$
$$a_4 = \frac{\tau_1 v_1(\psi_1 + \psi_2) + \omega^* v_1(\mu_1 + \tau_1 + \tau_2)}{(\mu_1 + \tau_1 + \tau_2)(\zeta + \delta + \mu_1 + \gamma + \theta)},$$
$$a_5 = \frac{\tau_1 v_1(\psi_1 + \psi_2) + \omega^* v_1(\mu_1 + \tau_1 + \tau_2)(\zeta - \zeta\xi)}{(\mu_1 + \tau_1 + \tau_2)\mu_2(\zeta + \delta + \mu_1 + \gamma + \theta)},$$
$$a_6 = \frac{\psi_1 + \psi_2}{\mu_1 + \tau_1 + \tau_2},$$
$$a_7 = \left(\frac{\psi_1 + \psi_2}{\mu_1 + \tau_1 + \tau_2}\right)^2,$$
$$a_8 = \frac{\psi_1 + \psi_2}{\mu_1 + \tau_1 + \tau_2} \frac{\tau_1 v_1(\psi_1 + \psi_2) + \omega^* v_1(\zeta + \delta + \mu_1 + \gamma + \theta)}{(\mu_1 + \tau_1 + \tau_2)(\zeta + \delta + \mu_1 + \gamma + \theta)},$$
$$a_9 = \frac{\psi_1 + \psi_2}{\mu_1 + \tau_1 + \tau_2} \frac{\tau_1 v_1(\psi_1 + \psi_2) + \omega^* v_1(\zeta + \delta + \mu_1 + \gamma + \theta)}{(\mu_1 + \tau_1 + \tau_2)(\zeta + \delta + \mu_1 + \gamma + \theta)},$$
$$a_{10} = \frac{\psi_1 + \psi_2}{\mu_1 + \tau_1 + \tau_2} \frac{\tau_1 v_1(\psi_1 + \psi_2) + \omega^* v_1(\mu_1 + \tau_1 + \tau_2)(\zeta - \zeta\xi)}{(\mu_1 + \tau_1 + \tau_2)\mu_2(\zeta + \delta + \mu_1 + \gamma + \theta)},$$
$$a_{11} = \frac{\tau_1 v_1(\psi_1 + \psi_2) + \omega^* v_1(\zeta + \delta + \mu_1 + \gamma + \theta)}{(\mu_1 + \tau_1 + \tau_2)(\zeta + \delta + \mu_1 + \gamma + \theta)},$$
$$a_{12} = \frac{\tau_1 v_1(\psi_1 + \psi_2) + \omega^* v_1(\zeta + \delta + \mu_1 + \gamma + \theta)}{(\mu_1 + \tau_1 + \tau_2)(\zeta + \delta + \mu_1 + \gamma + \theta)} \frac{\psi_1 + \psi_2}{\mu_1 + \tau_1 + \tau_2},$$
$$a_{13} = \left(\frac{\tau_1 v_1(\psi_1 + \psi_2) + \omega^* v_1(\zeta + \delta + \mu_1 + \gamma + \theta)}{(\mu_1 + \tau_1 + \tau_2)(\zeta + \delta + \mu_1 + \gamma + \theta)}\right)^2,$$
$$a_{14} = \frac{\tau_1 v_1(\psi_1+\psi_2)+\omega^* v_1(\zeta+\delta+\mu_1+\gamma+\theta)}{(\mu_1+\tau_1+\tau_2)(\zeta+\delta+\mu_1+\gamma+\theta)} \frac{\tau_1 v_1(\psi_1+\psi_2)+\omega^* v_1(\mu_1+\tau_1+\tau_2)}{(\mu_1+\tau_1+\tau_2)(\zeta+\delta+\mu_1+\gamma+\theta)},$$
$$a_{15} = \frac{\tau_1 v_1(\psi_1+\psi_2)+\omega^* v_1(\zeta+\delta+\mu_1+\gamma+\theta)}{(\mu_1+\tau_1+\tau_2)(\zeta+\delta+\mu_1+\gamma+\theta)} \frac{\tau_1 v_1(\psi_1+\psi_2)+\omega^* v_1(\mu_1+\tau_1+\tau_2)(\zeta-\zeta\xi)}{(\mu_1+\tau_1+\tau_2)\mu_2(\zeta+\delta+\mu_1+\gamma+\theta)},$$
$$a_{16} = \frac{\tau_1 v_1(\psi_1 + \psi_2) + \omega^* v_1(\mu_1 + \tau_1 + \tau_2)}{(\mu_1 + \tau_1 + \tau_2)(\zeta + \delta + \mu_1 + \gamma + \theta)},$$
$$a_{17} = \frac{\tau_1 v_1(\psi_1 + \psi_2) + \omega^* v_1(\mu_1 + \tau_1 + \tau_2)}{(\mu_1 + \tau_1 + \tau_2)(\zeta + \delta + \mu_1 + \gamma + \theta)} \frac{\psi_1 + \psi_2}{\mu_1 + \tau_1 + \tau_2},$$
$$a_{18} = \frac{\tau_1 v_1(\psi_1+\psi_2)+\omega^* v_1(\mu_1+\tau_1+\tau_2)}{(\mu_1+\tau_1+\tau_2)(\zeta+\delta+\mu_1+\gamma+\theta)} \frac{\tau_1 v_1(\psi_1+\psi_2)+\omega^* v_1(\zeta+\delta+\mu_1+\gamma+\theta)}{(\mu_1+\tau_1+\tau_2)(\zeta+\delta+\mu_1+\gamma+\theta)},$$
$$a_{19} = \left(\frac{\tau_1 v_1(\psi_1 + \psi_2) + \omega^* v_1(\mu_1 + \tau_1 + \tau_2)}{(\mu_1 + \tau_1 + \tau_2)(\zeta + \delta + \mu_1 + \gamma + \theta)}\right)^2,$$

ETNA
Kent State University and
Johann Radon Institute (RICAM)

$$a_{20} = \frac{\tau_1 v_1(\psi_1+\psi_2)+\omega^* v_1(\mu_1+\tau_1+\tau_2)}{(\mu_1+\tau_1+\tau_2)(\zeta+\delta+\mu_1+\gamma+\theta)} \frac{\tau_1 v_1(\psi_1+\psi_2)+\omega^* v_1(\mu_1+\tau_1+\tau_2)(\zeta-\zeta\xi)}{(\mu_1+\tau_1+\tau_2)\mu_2(\zeta+\delta+\mu_1+\gamma+\theta)},$$
$$a_{21} = \frac{\tau_1 v_1(\psi_1+\psi_2)+\omega^* v_1(\mu_1+\tau_1+\tau_2)(\zeta-\zeta\xi)}{(\mu_1+\tau_1+\tau_2)\mu_2(\zeta+\delta+\mu_1+\gamma+\theta)},$$
$$a_{22} = \frac{\tau_1 v_1(\psi_1+\psi_2)+\omega^* v_1(\mu_1+\tau_1+\tau_2)(\zeta-\zeta\xi)}{(\mu_1+\tau_1+\tau_2)\mu_2(\zeta+\delta+\mu_1+\gamma+\theta)} \frac{\psi_1+\psi_2}{\mu_1+\tau_1+\tau_2},$$
$$a_{23} = \frac{\tau_1 v_1(\psi_1+\psi_2)+\omega^* v_1(\mu_1+\tau_1+\tau_2)(\zeta-\zeta\xi)}{(\mu_1+\tau_1+\tau_2)\mu_2(\zeta+\delta+\mu_1+\gamma+\theta)} \frac{\tau_1 v_1(\psi_1+\psi_2)+\omega^* v_1(\zeta+\delta+\mu_1+\gamma+\theta)}{(\mu_1+\tau_1+\tau_2)(\zeta+\delta+\mu_1+\gamma+\theta)},$$
$$a_{24} = \frac{\tau_1 v_1(\psi_1+\psi_2)+\omega^* v_1(\mu_1+\tau_1+\tau_2)(\zeta-\zeta\xi)}{(\mu_1+\tau_1+\tau_2)\mu_2(\zeta+\delta+\mu_1+\gamma+\theta)} \frac{\tau_1 v_1(\psi_1+\psi_2)+\omega^* v_1(\mu_1+\tau_1+\tau_2)}{(\mu_1+\tau_1+\tau_2)(\zeta+\delta+\mu_1+\gamma+\theta)},$$
$$a_{25} = \Big(\frac{\tau_1 v_1(\psi_1+\psi_2)+\omega^* v_1(\mu_1+\tau_1+\tau_2)(\zeta-\zeta\xi)}{(\mu_1+\tau_1+\tau_2)\mu_2(\zeta+\delta+\mu_1+\gamma+\theta)}\Big)^2.$$

Now,

$$A^T = \begin{bmatrix} b-\mu_1-\omega^*-\psi_1-\psi_2 & \psi_1+\psi_2 & \omega^* & 0 & 0 \\ 0 & -\mu_1-\tau_1-\tau_2 & \tau_1 & \tau_2 & 0 \\ 0 & 0 & -(\zeta+\delta+\mu_1+\gamma+\theta) & \gamma+\theta+\zeta\xi & \zeta-\zeta\xi \\ 0 & 0 & 0 & -\mu_1 & 0 \\ 0 & 0 & 0 & 0 & -\mu_2 \end{bmatrix}.$$

Assume that $w = (\omega_1, \omega_2, \omega_3, \omega_4, \omega_5)^T$ is an eigenvector of A^T corresponding to the eigenvalue 0:

$$A^T \begin{bmatrix} \omega_1 \\ \omega_2 \\ \omega_3 \\ \omega_4 \\ \omega_5 \end{bmatrix} = \begin{bmatrix} 0 \\ 0 \\ 0 \\ 0 \\ 0 \end{bmatrix}.$$

Thus,

$$\begin{aligned} (b-\mu_1-\omega^*-\psi_1-\psi_2)\omega_1 + (\psi_1+\psi_2)\omega_2 + \omega^*\omega_3 = 0 \quad \text{(a)},\\ (-\mu_1-\tau_1-\tau_2)\omega_2 + \tau_1\omega_3 + \tau_2\omega_4 = 0 \quad \text{(b)},\\ -(\zeta+\delta+\mu_1+\gamma+\theta)\omega_3 + (\gamma+\theta+\zeta\xi)\omega_4 + (\zeta-\zeta\xi)\omega_5 = 0 \quad \text{(c)},\\ -\mu_1\omega_4 = 0 \quad \text{(d)},\\ -\mu_2\omega_5 = 0 \quad \text{(e)}. \end{aligned}$$

From (c), (d), and (e), we obtain

$$\omega_3 = \omega_5 = 0,$$

and

$$\omega_1 = -\frac{(\psi_1+\psi_2)\omega_2}{b-\mu_1+\omega^*-\psi_1-\psi_2}, \qquad \omega_4 = \frac{(\mu_1+\tau_1+\tau_2)\omega_2}{\tau_2}.$$

Hence, the eigenvector w can be written as

$$w = \left[-\frac{(\psi_1+\psi_2)\omega_2}{b-\mu_1+\omega^*-\psi_1-\psi_2},\ \omega_2,\ 0,\ \frac{(\mu_1+\tau_1+\tau_2)\omega_2}{\tau_2},\ 0\right]^T.$$

ETNA
Kent State University and
Johann Radon Institute (RICAM)

$$f_\mu(x,\mu) = \begin{bmatrix} -S \\ 0 \\ S \\ 0 \\ 0 \end{bmatrix}, \qquad f_\mu(x_0,\mu_0) = \begin{bmatrix} 0 \\ 0 \\ 0 \\ 0 \\ 0 \end{bmatrix}$$

$$Df_\mu(x,\mu) = \begin{bmatrix} -1 & 0 & 0 & 0 & 0 \\ 0 & 0 & 0 & 0 & 0 \\ 1 & 0 & 0 & 0 & 0 \\ 0 & 0 & 0 & 0 & 0 \\ 0 & 0 & 0 & 0 & 0 \end{bmatrix}, \qquad Df_\mu(x_0,\mu_0) = \begin{bmatrix} -1 & 0 & 0 & 0 & 0 \\ 0 & 0 & 0 & 0 & 0 \\ 1 & 0 & 0 & 0 & 0 \\ 0 & 0 & 0 & 0 & 0 \\ 0 & 0 & 0 & 0 & 0 \end{bmatrix}.$$

a)

$$w^T f_\mu(x_0,\mu_0) = \left(\frac{-(\psi_1+\psi_2)\omega_2}{(b-\mu_1+\omega^*-\psi_1-\psi_2)}, \omega_2, 0, \frac{(\mu_1+\tau_1+\tau_2)\omega_2}{\tau_2}, 0 \right) \begin{bmatrix} 0 \\ 0 \\ 0 \\ 0 \\ 0 \end{bmatrix} = 0.$$

b)

$$\begin{aligned} & w^T[Df_\mu(x_0,\mu_0)V] \\ &= \left[\frac{-(\psi_1+\psi_2)\omega_2}{(b-\mu_1+\omega^*-\psi_1-\psi_2)}, \omega_2, 0, \frac{(\mu_1+\tau_1+\tau_2)\omega_2}{\tau_2}, 0 \right] \\ &\quad \times \left[\begin{bmatrix} -1 & 0 & 0 & 0 & 0 \\ 0 & 0 & 0 & 0 & 0 \\ 1 & 0 & 0 & 0 & 0 \\ 0 & 0 & 0 & 0 & 0 \\ 0 & 0 & 0 & 0 & 0 \end{bmatrix} \begin{bmatrix} 1 \\ \frac{\psi_1+\psi_2}{\mu_1+\tau_1+\tau_2} \\ \frac{\tau_1 v_1(\psi_1+\psi_2)+\omega^* v_1(\zeta+\delta+\mu_1+\gamma+\theta)}{(\mu_1+\tau_1+\tau_2)(\zeta+\delta+\mu_1+\gamma+\theta)} \\ \frac{\tau_1 v_1(\psi_1+\psi_2)+\omega^* v_1(\mu_1+\tau_1+\tau_2)}{(\mu_1+\tau_1+\tau_2)(\zeta+\delta+\mu_1+\gamma+\theta)} \\ \frac{\tau_1 v_1(\psi_1+\psi_2)+\omega^* v_1(\mu_1+\tau_1+\tau_2)(\zeta-\zeta\xi)}{(\mu_1+\tau_1+\tau_2)\mu_2(\zeta+\delta+\mu_1+\gamma+\theta)} \end{bmatrix} \right] \\ &= \frac{(\psi_1+\psi_2)\omega_2}{(b-\mu_1+\omega^*-\psi_1-\psi_2)} \neq 0. \end{aligned}$$

c)

$$\begin{aligned} & w^T[D^2 f(x_0,\mu_0)(v,v)] \\ &= \left[\frac{-(\psi_1+\psi_2)\omega_2}{(b-\mu_1+\omega^*-\psi_1-\psi_2)}, \omega_2, 0, \frac{(\mu_1+\tau_1+\tau_2)\omega_2}{\tau_2}, 0 \right] \\ &\quad \times \begin{bmatrix} \frac{-2b}{K} - \frac{2\beta}{N}\left(\frac{\tau_1 v_1(\psi_1+\psi_2)+\omega^* v_1(\zeta+\delta+\mu_1+\gamma+\theta)}{(\mu_1+\tau_1+\tau_2)(\zeta+\delta+\mu_1+\gamma+\theta)}\right. \\ 0 \\ \frac{2\beta}{N}\frac{\tau_1 v_1(\psi_1+\psi_2)+\omega^* v_1(\zeta+\delta+\mu_1+\gamma+\theta)}{(\mu_1+\tau_1+\tau_2)(\zeta+\delta+\mu_1+\gamma+\theta)} \\ 0 \\ 0 \end{bmatrix} \\ &= \frac{-(\psi_1+\psi_2)\omega_2}{(b-\mu_1+\omega^*-\psi_1-\psi_2)} \\ &\quad \times \left(\frac{-2b}{K} - \frac{2\beta}{N}\left(\frac{\tau_1 v_1(\psi_1+\psi_2)+\omega^* v_1(\zeta+\delta+\mu_1+\gamma+\theta)}{(\mu_1+\tau_1+\tau_2)(\zeta+\delta+\mu_1+\gamma+\theta)}\right) \right) \neq 0. \end{aligned}$$

ETNA
Kent State University and
Johann Radon Institute (RICAM)

By Sotomayor's theorem, this tells us that the system (3.1) does exhibit a trans-critical bifurcation.

The bifurcation analysis with respect to the parameter ω provides further insight into the nonlinear behavior of the proposed fractional-order system. As shown in Figure 13.1, variations in ω lead to qualitative changes in the stability of the equilibrium branches, indicating the possible presence of both forward and backward bifurcation phenomena. In the forward bifurcation scenario, the disease-free equilibrium loses stability once the critical threshold is exceeded, giving rise to a unique endemic equilibrium. On the other hand, backward bifurcation suggests the coexistence of multiple equilibria even when the threshold parameter remains below unity, implying that disease elimination may not be achieved solely by reducing the reproduction threshold. This result highlights the impact of memory effects inherent in the fractional-order framework and their role in prolonging disease persistence and altering transition dynamics.

The presence of forward and backward bifurcations has important public health implications. In particular, backward bifurcation indicates that reducing the basic reproduction number below unity may not always be sufficient for disease eradication. This suggests that stronger intervention strategies, such as sustained vaccination campaigns and behavioral restrictions on aspirin use, may be required to eliminate persistent outbreaks.

Despite the effectiveness of the proposed framework, certain limitations should be acknowledged. The model assumes homogeneous mixing of the population and does not explicitly incorporate age structure, spatial heterogeneity, or stochastic fluctuations. Future research may focus on extending the model to include these factors for a more comprehensive epidemiological description.

The bifurcation diagram with respect to the parameter ω demonstrates the existence of a critical threshold that governs the qualitative behavior of the system. For lower values of ω, the disease-free equilibrium remains stable, indicating that the infection dies out over time. However, as ω increases beyond a critical value, the system undergoes a bifurcation, leading to the appearance of a stable endemic equilibrium. This indicates that behavioral factors and increased transmission pressure significantly contribute to disease persistence.

The bifurcation analysis with respect to the fractional order ϑ highlights the significant role of memory effects in the epidemic dynamics. Lower values of ϑ strengthen the memory effect of the system, leading to reduced infection levels and delayed outbreak intensity. In contrast, as ϑ approaches unity, the system behavior converges to the classical integer-order model, where the memory effect diminishes and the infection level increases. These results confirm that fractional-order modeling provides a more flexible and realistic framework for capturing complex epidemiological behavior.

Figure 13.2 presents the phase portrait of the epidemic model for three different initial conditions. It is observed that, regardless of the initial states, all trajectories converge to the same equilibrium point. This behavior indicates stability of the endemic equilibrium and confirms that the long-term dynamics of the system is independent of the initial population distributions. The convergence pattern also reflects the robustness of the model and the presence of strong attractor dynamics in the fractional-order epidemic system.

14. Conclusions. In this study, we developed and analyzed a fractional-order mathematical model that links measles transmission dynamics with the occurrence of Reye's syndrome associated with aspirin use. The model is formulated using the Caputo fractional derivative, which allows the representation of memory effects and nonlocal temporal interactions that classical integer-order models cannot capture. Existence, positivity, and boundedness of solutions were theoretically established, and the equilibrium points of the system were determined to investigate its stability structure. Using a fixed-point theorem, the existence of equilibrium

ETNA
Kent State University and
Johann Radon Institute (RICAM)

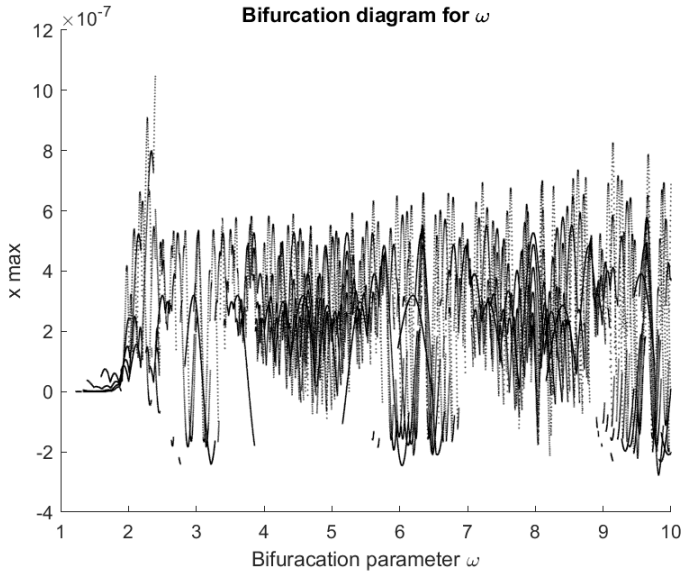

FIG. 13.1. *Bifurcation phase diagram with respect to the parameter* ω.

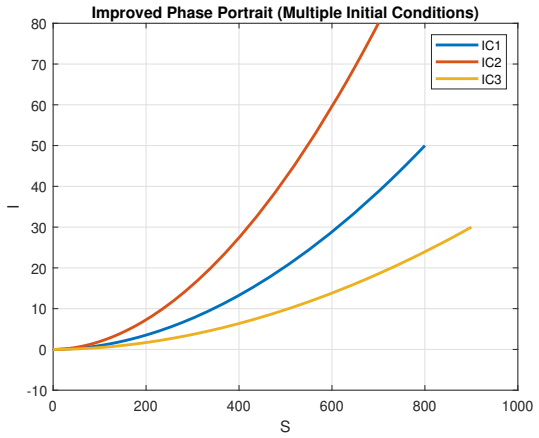

FIG. 13.2. *Phase portrait of the epidemic model for different initial conditions:* $IC_1 = (800, 100, 50, 20, 10)$, $IC_2 = (700, 150, 80, 30, 20)$, $IC_3 = (900, 50, 30, 10, 5)$. *The trajectories illustrate the dynamical behavior of the system in the* (S, I) *plane under varying initial states.*

solutions is demonstrated, and a stability analysis shows that the positive equilibrium remains asymptotically stable under appropriate parameter conditions. The findings indicate that although the equilibrium points of the fractional-order and integer-order models are identical, their dynamical behavior differs significantly. In particular, the fractional-order model exhibits slower convergence toward the equilibrium as ϑ decreases, reflecting stronger memory effects and prolonged disease persistence. Numerical simulations employed the Adams–Bashforth–Moulton predictor-corrector method for different values of the fractional order parameter ϑ and key epidemiological parameters.

ETNA
Kent State University and
Johann Radon Institute (RICAM)

The results confirm that decreasing ϑ intensifies memory effects, leading to delayed convergence and altered transient dynamics. As ϑ approaches unity, the system behavior converges to that of the classical integer-order model.

Calibration with real UK measles surveillance data demonstrate that the fractional-order framework provides improved fitting and a more realistic predictive performance compared with classical integer-order formulations. A scenario analysis further confirm that maintaining high MMR vaccination coverage and reducing aspirin use in febrile children can significantly decrease both measles incidence and the associated risk of Reye's syndrome.

Overall, the proposed model highlights the importance of incorporating memory effects, treatment behavior, and epidemiological data into infectious disease modeling. The results suggest that fractional-order models provide a more flexible and realistic framework for describing measles transmission and can offer valuable insights for public health decision-making.

Future research can further extend this framework to a broader class of infectious diseases by incorporating additional epidemiological complexities, including age-structured vaccination strategies, stochastic perturbations, and spatial transmission dynamics. Furthermore, integrating fractional-order modeling with advanced machine learning techniques offers a promising direction for improving parameter estimation, enhancing predictive accuracy, and capturing complex nonlinear patterns, while preserving the mechanistic interpretability and the theoretical rigor of the model. Such developments may provide a more robust and realistic framework for understanding disease progression and supporting public health decision-making.

REFERENCES

[1] M. A. M. ABDELAZIZ, A. I. ISMAIL, F. A. ABDULLAH, AND M. H. MOHD, *Codimension one and two bifurcations of a discrete-time fractional-order SEIR measles epidemic model with constant vaccination*, Chaos Solitons & Fractals, 140 (2020), Paper No. 110104, 14 pages.

[2] N. ABDUL, L. YAHYA, R. RESMAWAN, AND A. R. NUHA, *Dynamic analysis of the mathematical model of the spread of cholera with vaccination strategies*, Barekeng J. Ilmu Mat. Terapan, 16 (2022), pp. 281–292.

[3] I. AL-DARABSAH, *A time-delayed SVEIR model for imperfect vaccine with a generalized nonmonotone incidence and application to measles*, Appl. Math. Model., 91 (2021), pp. 74–92.

[4] L. J. S. ALLEN, *An Introduction to Mathematical Biology*, Pearson/Prentice Hall, Upper Saddle River, 2007.

[5] N. A. ALSHAMMARI, N. S. ALHARTHI, A. M. SAEED, A. KHAN, AND P. A. NAIK, *Numerical solutions of a fractional order SEIR epidemic model of measles under Caputo fractional derivative*, PLOS One, 20 (2025), Paper No. e0321089, 25 pages.

[6] A. S. ALSHEHRY, S. MUKHTAR, H. S. KHAN, AND R. SHAH, *Fixed-point theory and numerical analysis of an epidemic model with fractional calculus: exploring dynamical behavior*, Open Phys., 21 (2023), Paper No. 20230121, 14 pages.

[7] B. BANKAMP, C. HICKMAN, J.P. ICENOGLE, AND P. A. ROTA, *Successes and challenges for preventing measles, mumps and rubella by vaccination*, Curr. Opin. Virol., 34 (2019), pp. 110–116.

[8] A. B. CELESTINE, R. DERVISHI, A. K. AWASTHI, A. H. GANIE, H. BUÇKA, H. EMADIFAR, A. SMERAT, AND K. SHYAMSUNDER, *Fractional-order modeling of pneumonia transmission with vaccination, re-infection, and data fitting to England cases*, Discover Public Health, 23 (2026), Paper No. 290, 38 pages.

[9] A. N. CHATTERJEE, S. K. SHARMA, AND F. AL BASIR, *A compartmental approach to modeling the measles disease: a fractional order optimal control model*, Fractal Fract., 8 (2024), Paper No. 446, 14 pages.

[10] N. CHITNIS, J. M. HYMAN, AND J. M. CUSHING, *Determining important parameters in the spread of malaria through the sensitivity analysis of a mathematical model*, Bull. Math. Biol., 70 (2008), pp. 1272–1296.

[11] A. DAS, K. DEHINGIA, E. HINÇAL, F. ÖZKÖSE, AND K. HOSSEINI, *A study on the dynamics of a breast cancer model with discrete-time delay*, Phys. Scr., 99 (2024), Paper No. 035235, 20 pages.

[12] K. DIETHELM, *An algorithm for the numerical solution of differential equations of fractional order*, Electron. Trans. Numer. Anal., 5 (1997), pp. 1–6.
https://etna.ricam.oeaw.ac.at/vol.5.1997/pp1-6.dir/pp1-6.pdf

[13] K. DIETHELM AND A. D. FREED, *The FracPECE subroutine for the numerical solution of differential equations of fractional order*, in Forschung und Wissenschaftliches Rechnen 1998, GWDG-Bericht, S. Heinzel and T. Plesser, eds., Gesellschaft für Wissenschaftliche Datenverarbeitung, Göttingen, 1999,

ETNA
Kent State University and
Johann Radon Institute (RICAM)

pp. 57–71.

[14] C. A. DIMALA, B. M. KADIA, M. A. M. NJI, AND N. N. BECHEM, *Factors associated with measles resurgence in the United States in the post-elimination era*, Sci. Rep., 11 (2021). https://doi.org/10.1038/s41598-020-80214-3

[15] M. EL HAJJI AND A. H. ALBARGI, *A mathematical investigation of an SVEIR epidemic model for the measles transmission*, Math. Biosci. Eng., 19 (2022), pp. 2853–2875.

[16] A. EL-MESADY, A. M. S. MAHDY, AND F. ÖZKÖSE, *A fractional-order model with prevention and isolation optimal control measures to reduce the transmission of Tuberculosis*, J. Taibah Univ. Sci., 19 (2025), Paper No. 2475579, 23 pages.

[17] R. GARRAPPA, *On linear stability of predictor-corrector algorithms for fractional differential equations*, Int. J. Comput. Math., 87 (2010), pp. 2281–2290.

[18] ———, *Numerical solution of fractional differential equations: a survey and a software tutorial*, Mathematics, 6 (2018), 16 pages. https://doi.org/10.3390/math6020016

[19] R. K. GHAZIANI, J. ALIDOUSTI, AND A. B. ESHKAFTAKI, *Stability and dynamics of a fractional order Leslie-Gower prey-predator model*, Appl. Math. Model., 40 (2016), pp. 2075–2086.

[20] J. A. GOSALAKKAL AND V. KAMOJI, *Reye syndrome and Reye-like syndrome*, Pediatr. Neurol., 39 (2008), pp. 198–200.

[21] C. HUANG, X. SONG, B. FANG, M. XIAO, AND J. CAO, *Modeling, analysis and bifurcation control of a delayed fractional-order predator-prey model*, Int. J. Bifurcation Chaos, 28 (2018), Paper No. 1850117.

[22] S. JAMIL, P. A. NAIK, M. FARMAN, M. U. SALEEM, AND A. H. GANIE, *Stability and complex dynamical analysis of COVID-19 epidemic model with non-singular kernel of Mittag-Leffler law*, J. Appl. Math. Comput., 70 (2024), pp. 3441–3476.

[23] A. S. KU AND L. T. CHAN, *The first case of H5N1 avian influenza infection in a human with complications of adult respiratory distress syndrome and Reye's syndrome*, J. Paediatr. Child Health, 35 (1999), pp. 207–209.

[24] I. S. KUSMAWATI AND T. D. CHANDRA, *Stability analysis of SIRS epidemic model on measles disease spreading with vaccination and migration*, J. Phys. Conf. Ser., 1872 (2021), Paper No. 012033, 7 pages.

[25] C. LI AND C. TAO, *On the fractional Adams method*, Comput. Math. Appl., 58 (2009), pp. 1573–1588.

[26] B. MUGOŠA, G. CECCARELLI, S. BEGIĆ, D. VUJOŠEVIĆ, Z. ZEKOVIC, M. CICCOZZI, AND Z. VRATNICA, *Measles outbreak, Montenegro January–July 2018: lessons learned*, J. Med. Virol., 94 (2021), pp. 514–520.

[27] P. A. NAIK, Y. JAVAID, R. AHMED, Z. ESKANDARI, AND A. H. GANIE, *Stability and bifurcation analysis of a population dynamic model with Allee effect via piecewise constant argument method*, J. Appl. Math. Comput., 70 (2024), pp. 4189–4218.

[28] P. A. NAIK, B. S. N. MURTHY, M. N. SRINIVAS, L. CHADA, M. N. RAJU, AND D. V. SARADHI, *Exploring the dynamics of rabies epidemic model using Caputo–Fabrizio derivative under treatment and vaccination*, Comput. Methods Biomech. Biomed. Eng., (2026), pp. 1–19. https://doi.org/10.1080/10255842.2026.2613116

[29] D. NUWAHEREZE, M. O. ONUORAH, B. M. ABDULAHI, AND I. KABANDANA, *Standard incidence model of measles with two vaccination strategies*, World Sci. News, 170 (2022), pp. 149–171.

[30] F. ÖZKÖSE, *Modeling of psoriasis by considering drug influence: a mathematical approach with memory trace*, Comput. Biol. Med., 168 (2024), Paper No. 107791, 22 pages.

[31] F. ÖZKÖSE, M.T. ŞENEL, AND R. HABBIREEH, *Fractional-order mathematical modelling of cancer cells-cancer stem cells-immune system interaction with chemotherapy*, Math. Model. Numer. Simul. Appl., 1 (2021), pp. 67–83.

[32] F. ÖZKÖSE, S. YILMAZ, M. T. ŞENEL, M. YAVUZ, S. TOWNLEY, AND M. DOĞAN SARIKAYA, *A mathematical modeling of patient-derived lung cancer stem cells with fractional-order derivative*, Phys. Scr., 99 (2024), Paper No. 115235, 20 pages.

[33] F. ÖZKÖSE, R. HABBIREEH, AND M.T. ŞENEL, *A novel fractional order model of SARS-CoV-2 and cholera disease with real data*, J. Comput. Appl. Math., 423 (2023), Paper No. 114969, 29 pages.

[34] J. P. ORLOWSKI, U. A. HANHAN, AND M. R. FIALLOS, *Is aspirin a cause of Reye's syndrome? A case against*, Drug Saf., 25 (2002), pp. 225–231.

[35] I. PETRÁŠ, *Fractional-Order Nonlinear Systems*, Springer, Berlin, 2011.

[36] I. PODLUBNY, *Fractional Differential Equations*, Academic Press, San Diego, 1999.

[37] A. PORTER AND J. GOLDFARB, *Measles: a dangerous vaccine-preventable disease returns*, Cleve Clin. J. Med., 86 (2019), pp. 393–398.

[38] D. RUDERFER AND L.R. KRILOV, *Vaccine-preventable outbreaks: still with us after all these years*, Pediatr. Ann., 44 (2015), pp. e76–e81.

[39] Y. SABBAR, M. YAVUZ, AND F. ÖZKÖSE, *Infection eradication criterion in a general epidemic model with logistic growth, quarantine strategy, media intrusion, and quadratic perturbation*, Mathematics, 10 (2022), Paper No. 4213, 16 pages.

ETNA
Kent State University and
Johann Radon Institute (RICAM)

[40] D. N. SINHA, N. KLAHN, AND S. PEHLIVAN, *Mathematical modeling of the 2019 measles outbreak on US population*, Acta Sci. Microbiol., 3 (2022), pp. 209–214.

[41] P. VAN DEN DRIESSCHE AND J. WATMOUGH, *Reproduction numbers and sub-threshold endemic equilibria for compartmental models of disease transmission*, Math. Biosci., 180 (2002), pp. 29–48.

[42] M. XIAO, W. X. ZHENG, G. JIANG, AND J. CAO, *Undamped oscillations generated by Hopf bifurcations in fractional-order recurrent neural networks with Caputo derivative*, IEEE Trans. Neural Netw. Learn. Syst., 26 (2015), pp. 3201–3214.